Water Resources Research

RESEARCH ARTICLE
10.1029/2024WR037742

Sediment Transport and Flood Risk: Impact of Newly Constructed Embankments on River Morphology and Flood Dynamics in Kathmandu, Nepal

Saraswati Thapa[1,2], Hugh D. Sinclair[1], Maggie J. Creed[3], Alistair G. L. Borthwick[4,5], C. Scott Watson[6], and Manoranjan Muthusamy[7]

[1]School of Geosciences, University of Edinburgh, Edinburgh, UK, [2]Pulchowk Campus, Institute of Engineering, Tribhuvan University, Lalitpur, Nepal, [3]James Watt School of Engineering, University of Glasgow, Glasgow, UK, [4]School of Engineering, University of Edinburgh, Edinburgh, UK, [5]School of Engineering, Computing and Mathematics, University of Plymouth, Plymouth, UK, [6]COMET, School of Earth and Environment, University of Leeds, Leeds, UK, [7]FloodFlash, London, UK

Abstract Floodplain encroachment by embankments heightens flood risk. This is exacerbated by climate change and land-use modifications. This paper assesses the impact of embankments on sediment transport, channel geometry, conveyance capacity, and flood inundation of a reach of the Nakkhu River, Nepal. Using the CAESAR-Lisflood landscape evolution model based on a 2-m digital elevation model, we simulate four flood scenarios with and without embankments and sediment transport: a historical 25-year return period flood event used to design the embankments, 50-year, 100-year, and 1000-year return period flood events forecast using the Generalized Logistic Model (using data from 1992 to 2017). Our results indicate that flow confinement by embankments reduces inundation by 99% (from 22.5 to 0.3 ha) for the historical 25-year flood discharge of 42.23 m^3/s and by 15% (from 28.8 to 24.4 ha) for the 1000-year return period flood discharge of 95 m^3/s (similar to a 25-year maximum mid-future). The presence of embankments increases downstream sediment transport by more than 32% for all flood scenarios considered. Inclusion of sediment transport leads to a fivefold increase in predicted inundation area for a 25-year maximum mid-future flood compared to the no-sediment case in the embanked channel. Changes in channel geometry due to sedimentation significantly reduce conveyance capacity increasing overtopping flood risk, particularly where the channel is sinuous or located on flat terrain. Our results indicate that sediment erosion in outer meanders may threaten embankment stability by promoting undercuts. It is recommended that sediment transport effects be factored into embankment design and floodplain planning.

Plain Language Summary Our research explores the impact of flood protection embankments being constructed along the Nakkhu River in the Kathmandu Valley, Nepal, in a region that is experiencing rapid urban growth. Using advanced computer simulations, we study how these embankments influence the erosion and deposition of sediment in the river, and hence impact flood risk. Our findings indicate that the construction of embankments increases sediment transport, and alters the geometry of the river increasing downstream flood risk during extreme flood events. This is particularly the case for embankments designed to follow natural, meandering river courses. We recommend incorporating sediment transport analysis into the planning and design of embankments and developments in floodplain areas to reduce the risk of flooding. Our study indicates that embankment construction by itself may not always be a sustainable long-term flood-protection measure for rivers carrying high sediment loads.

Key Points:

- Inclusion of sediment processes is very important in predicting the effect of embankments on river flood risk
- For the embanked Nakkhu, predicted inundation is fivefold larger for 25-year maximum mid-future event when sediment transport is included
- Sedimentation reduces channel capacity for flat terrain and large meanders; erosion at outer meanders threatens Nakkhu embankment stability

Supporting Information:

Supporting Information may be found in the online version of this article.

Correspondence to:

S. Thapa,
saraswati.thapa@ed.ac.uk

Citation:

Thapa, S., Sinclair, H. D., Creed, M. J., Borthwick, A. G. L., Watson, C. S., & Muthusamy, M. (2024). Sediment transport and flood risk: Impact of newly constructed embankments on river morphology and flood dynamics in Kathmandu, Nepal. *Water Resources Research*, *60*, e2024WR037742. https://doi.org/10.1029/2024WR037742

Received 17 APR 2024
Accepted 7 OCT 2024

Author Contributions:

Conceptualization: Saraswati Thapa, Hugh D. Sinclair, Maggie J. Creed, Alistair G. L. Borthwick
Data curation: Saraswati Thapa, C. Scott Watson, Manoranjan Muthusamy
Formal analysis: Saraswati Thapa
Funding acquisition: Hugh D. Sinclair
Investigation: Saraswati Thapa, Hugh D. Sinclair, Maggie J. Creed
Methodology: Saraswati Thapa
Project administration: Hugh D. Sinclair
Resources: Saraswati Thapa, Hugh D. Sinclair
Software: Saraswati Thapa

1. Introduction

Flood disasters are ubiquitous, frequent, and often catastrophic, causing significant damage to property and human life. During the last quarter of the twentieth century, floods contributed to almost half of the worldwide natural disaster fatalities (Berz, 2000; Doocy et al., 2013). About 1.81 billion individuals, accounting for 23% of the global population, face direct exposure to 1-in-100-year floods; among these, 1.24 billion reside in South and East Asia (Rentschler et al., 2022). The magnitude and frequency of flood disasters are influenced by climate change, alterations in land use, and anthropogenic activities (Arnell & Gosling, 2016; C. Ouellet & Normand, 2012; Hirabayashi et al., 2013; Kron, 2015; Li-An et al., 2018; Yang et al., 2021). Climate change and land-use modifications also affect sediment flux and grain size delivered to rivers (H. Li et al., 2022; Kido et al., 2023).

Supervision: Hugh D. Sinclair, Maggie J. Creed, Alistair G. L. Borthwick
Validation: Saraswati Thapa, Maggie J. Creed
Visualization: Saraswati Thapa, Hugh D. Sinclair, Maggie J. Creed
Writing – original draft: Saraswati Thapa
Writing – review & editing: Saraswati Thapa, Hugh D. Sinclair, Maggie J. Creed, Alistair G. L. Borthwick, C. Scott Watson, Manoranjan Muthusamy

Recent studies emphasize that sediment transport and morphological change processes have fundamental effects on flood hazards, with extreme floods significantly altering river morphology and channel capacity, thereby influencing future flood risk (Ahrendt et al., 2022; Guan et al., 2016; Lane et al., 2007; Raven et al., 2010; Slater et al., 2015; S. Thapa, Sinclair, Creed, Mudd, et al., 2024; Vázquez-Tarrío et al., 2023). For rivers in Western Washington State, US, channel conveyance variability related to sediment supply was found to have a greater effect on flood risk than stream flow variability (Ahrendt et al., 2022; Pfeiffer et al., 2019). The effect was larger for regulated rivers, highlighting the need to account for channel conveyance variability in flood hazard forecasting. Kido et al. (2023) estimated that a modest increase in precipitation (of approximately 1.2–1.6 times current levels) caused by climate change, could result in a substantial 3–5.5 fold increase in sediment discharge of the Pekerebetsu River, Japan. This, in turn, alters channel morphology and modifies flood risk (see e.g. S. Thapa, Sinclair, Creed, Mudd, et al. (2024)). In a review of flood disaster studies for Himalayan rivers, Sharma et al. (2019) emphasized river morphology change as a prevalent challenge in flood disaster management. High mountain catchments are notoriously susceptible to morphological change due to changes in hillslope sediment supply (Michaelides & Singer, 2014; Montgomery & Buffington, 1997). The rivers in such catchments can also carry substantial sediment loads, exacerbating downstream flood risk by accelerating sediment deposition in the plains (Leopold et al., 2020).

Over hundreds of years, embankments and flood walls have been used worldwide for flood protection, particularly in urban areas. However, these constructions may alter the natural capacity of the main channel to move sediment, causing erosion and deposition in different places. In the past, the potential consequences of embankment construction on morphological change processes were often overlooked during the planning phase, resulting in substantial recurrent maintenance costs (Fisher, 1992). In practice, embankments narrow the natural channel width and prevent overbank flow up to a design limit, while increasing conveyance capacity and stream power. In turn, embankments can significantly increase the rate of geomorphic change, with greater local erosion and sediment transport occurring during high flows (Cea & Costabile, 2022; McCann, 2013) and sedimentation at locations with low flow conditions. For example, the Brahmaputra Right Embankment in Bangladeshhas undergone erosion with reconstruction activities repeated nearly 10 times in the past 50 years (Oberhagemann et al., 2020). The construction of tall embankments (Figure 1) for flood protection measures is costly and may worsen flood risk by promoting sedimentation in the main channel leading to a perched riverbed. Examples include the Koshi River in Nepal and the Yellow River in China. The Yellow River's embankments have trapped so much silt that at certain locations the river bed is 6 m higher than the surrounding land (G. Li, 2003; World Bank, 2014). Moreover, the presence of embankments may create a false sense of security, promoting unchecked construction of houses and infrastructure which are vulnerable to extreme floods, as shown in Figure 1 (World Bank, 2014). Although much effort has been placed on hydraulic analysis for river structure design (see e.g. Morris, Hanson, and Hassan (2008); Morris, Hassan, et al. (2008)), relatively little attention has been given to the interaction between hydrodynamics, sediment transport, and performance of river structures for flood protection (Morris, Hanson, & Hassan, 2008), challenging the assumption of constant river geometry in flood models used in the design of flood control structures. There is clearly an urgent need to reconsider comprehensive flood risk management and engineering design.

The United Nations (2019) predicts an approximately 68% increase in global urban population between 2018 and 2050, with ~90% in developing nations in Asia and Africa. The global percentage of urban population was 50% in 2007 and 56% in 2020. Nepal is a rapidly urbanizing country that has sustained an average annual urban growth of 4% from 1961 to 2017, with the proportion of urban population reaching 22.7% in 2018 (United Nations, 2019). This urbanization trend is leading to the expansion of cities and human settlements into floodplains and flood-prone areas (Dixit & Shaw, 2023; Khanal et al., 2019). In recent years, Kathmandu, the capital city of Nepal, has undergone substantial urbanization driven by rural-to-urban migration (seeking enhanced access to education, healthcare, and services), significant changes in land use, infrastructure development, and the Nepal government's strategic plans to establish smart cities along the city's outer ring road (Timsina et al., 2020). Wang et al. (2020) showed that over two decades (1990–2010), Kathmandu has witnessed a decline of 9.28% in forest cover, 9.80% in agricultural land, and a 77% reduction in surface area of its water bodies. The Nepali government has been facing major challenges in implementing the plans strategically while incorporating rapid changes in land-use patterns (Muzzini & Aparicio, 2013).

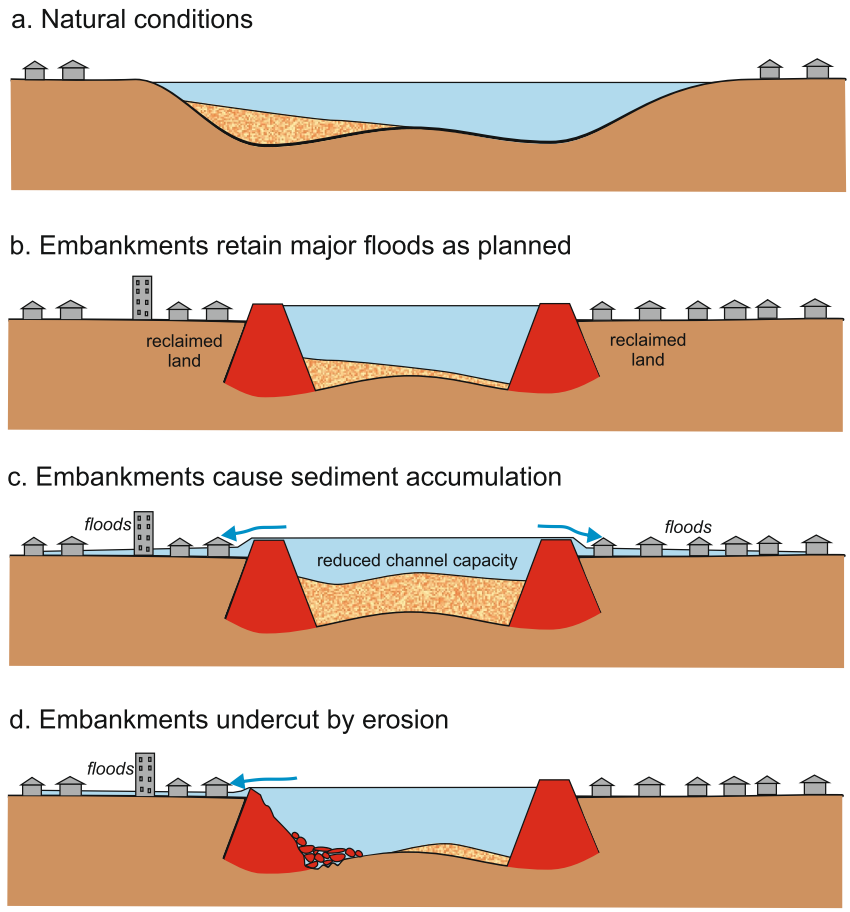

Figure 1. Sketches illustrate typical river channel cross-sections before and after the construction of embankments: (a) natural river cross-section scenario without embankment where water flows through a broad area with few temporary settlements; (b) situation after embankment construction, depicting an increased settlement of people near the embankment to the flood plain, experiencing raised water levels and risk of embankment overtopping or breaching; (c) scenario a few years after embankment construction, showing locations with sedimentation reducing channel capacity, leading to embankment overtopping and flooding; and (d) condition a few years after embankment construction, depicting locations with sediment erosion causing embankment undercutting that threatens embankment stability and raises flood risk.

Presently, Kathmandu accounts for one-twelfth of Nepal's total population. The city has a population density of approximately 20,288 persons/km^2 (see world population review on https://worldpopulationreview.com/world-cities/kathmandu-population). The combined effect of land-use change caused by recent urbanization and climate change have had a major impact on the hydrological regime of the Kathmandu Valley watershed (Lamichhane & Shakya, 2019; Shrestha et al., 2023). The primary causes of flooding in the Kathmandu Valley are fluvial flooding due to the Bagmati river and its tributaries running through the city, urban pluvial flooding caused by monsoon rainfall, alterations in land use, and inadequate drainage systems (Chaulagain et al., 2023). The increase in regional impervious surface area has resulted in reduced hydrologic response times and elevated flood risk in the city (Feng et al., 2021). Analysis of the Kathmandu Valley land-use maps from 1989 to 2016 revealed a 412% increase in built-up areas, potentially causing more than a 200% increase in stormwater runoff (Ishtiaque et al., 2017). Land-use changes have also impacted sediment yield in the Bagmati River (Pokhrel, 2018). If the current trend in urbanization of the urban and peri-urban areas of Kathmandu Valley persists, most of the remaining land resources, such as open spaces, river banks, forest, and fertile agriculture land, will be incorporated into built-up areas by 2050 (R. B. Thapa & Murayama, 2012). This rapid urbanization in Kathmandu, especially in embankment-protected river areas (Figure 1), presents a major challenge for the management of future flood risk.

In Nepal, river embankments are widely used for flood protection purposes, especially in areas subject to rapid urbanization, river training (narrowing) schemes, and sand and gravel extraction. However, urban development of

the floodplain and the vulnerability of embankments to breaching, overtopping, and seepage have raised questions as to whether such embankments offer appropriate long-term sustainable protection against future floods (Dixit, 2009). It has been suggested that even well-executed watershed conservation efforts may not sufficiently reduce river sediment yields to levels manageable for embankments in rivers such as the Koshi River (Gill & Paswan, 17 August 2018). In 2008, when the Koshi River breached its embankment, the riverbed within the embankment was approximately 4 m higher than the adjacent land, indicating an elevation increase of around 1 m every decade following the construction of the embankments (Devkota et al., 2012; Dixit, 2009; World Bank, 2014). Following the 2008 Koshi event, Dixit (2009) concluded that a paradigm shift was necessary in the traditional flood control and management techniques then implemented in Nepal. Bhatt et al. (2010) recommended consistent monitoring of river morphology changes, channel aggradation, and potential embankment threats, and advised the use of remote sensing techniques such as satellite imagery by planners in devising and implementing essential measures for channel stabilization and embankment reinforcement. Over the past 25 years, global flood management trends have shifted from implementing fixed flood control measures toward continuous adaptation that integrates global resilience and sustainability principles (Lihong et al., 2022). This shift is urgently needed in the context of urban planning and policy in Nepal to reduce flood risk caused by rapid urbanization and river encroachment (Wang et al., 2020). Although recent global-scale coarse-resolution flood modeling and flood assessments (Alfieri et al., 2017; Dottori et al., 2018; Pekel et al., 2016; Sampson et al., 2015; Smith et al., 2015; Ward et al., 2013; Zischg & Bermúdez, 2020) have been helpful to analyze flood risk in large river systems (e.g., Flood Hazard Map in Meteor Explorer on https://maps.meteor-project.org/map/flood-npl/#8/27.631/84.150), they do not capture the localized flood impacts in small rivers that pass through urban regions or are embanked like the rivers in the Kathmandu Valley. It is imperative to simulate the effect of changes to hydrological and morphological processes on flood dynamics correctly using higher-resolution digital topography when developing comprehensive flood models to ensure more reliable flood maps and hydraulic calculations for natural and regulated river channels.

In Nepal, river sediment dynamics significantly impact flood risk, being influenced by extreme weather, diverse topography, and the fragile, young geological formation of the Himalaya. The mountainous terrain leads to high sediment loads from landslides and erosion, intensified by heavy rainfall (Sinha et al., 2019). These sediment loads alter river channels through enhanced deposition in alluvial systems, increasing flood risk by reducing channel capacity and leading to breaches of flood protection embankments (Sinha, 2008; Sinha et al., 2019). For example, during a moderate flood event on 18 August 2008, the course of the Koshi River shifted about 120 km eastward due to breaching of its eastern embankment 12 km upstream of a barrage (Sinha, 2008). The riverbed was observed to be 4–5 m higher than the surrounding floodplain level due to sediment aggradation (Sinha, 2008). In a study of historical channel migration in the Koshi River, Chakraborty et al. (2010) found that the thalweg oscillated randomly rather than undergoing unidirectional migration. Dixit (2009) suggested that the huge sediment transport of the Koshi River, about 120 million m^3 per year (95% during monsoon), poses a major risk to existing and proposed conventional flood control structures such as dams and embankments, indicating a need for a paradigm shift when dealing with flood risk. For the Karnali River in the Terai region of Nepal, Dingle et al. (2020) predicted that flood events carrying large sediment loads could aggrade the river bed causing the river to migrate across the densely populated alluvial river system and its floodplains. Dingle et al. (2020) recommended that bed elevation field measurements should be carried out after a major sediment-generating flood event, and the data used to update the Digital Elevation Model (DEM) and thus improve future flood estimates for Nepal. Dingle et al. (2020) found that flood inundation extent was greatly affected by changes in bed elevation during a 20-year return-period flood event. Turning to the Melamchi-Indrawati rivers, the hyper-concentrated sediment-laden debris flow event of 15 June 2021 caused an approximately four-fold increase in exposed gravel along a 30 km reach and up to 12 m of channel aggradation (Graf et al., 2023; Maharjan et al., 2021). In a previous study Chakraborty et al. (2010) recommended investigating the impact of engineered rivers whose flood protection works, including embankments, affect sediment transport and natural river courses. Moreover, the impact of sediment movement during multiple extreme floods on future flood hazards in Himalayan rivers remains largely unexplored (Dingle et al., 2020; Guan et al., 2016; Stover & Montgomery, 2001). There is considerable evidence that hydraulic structures, such as embankments, dams, and irrigation canals, can alter sediment movement within a channel, modify channel geometry (e.g., Bettes (2008); Dixit (2009)), and change flood patterns (e.g., Hudson et al. (2008); Ramirez et al. (2020)).

With rapid urbanization encroaching on floodplains, the construction of embankments in many developing countries has significantly altered natural river courses. The Nakkhu River in the Kathmandu Valley exemplifies the impact of such interventions on sediment transport and flood inundation. Previous research by S. Thapa, Sinclair, Creed, Mudd, et al. (2024) on the natural course of the Nakkhu River before embankment construction has highlighted the importance of sediment transport, especially given the increased variability in sediment supply from upstream sources owing to mining activities and landslides. The present study investigates how newly constructed embankments that are intended to reduce flood risk, modify sediment transport, channel geometry, conveyance capacity, and consequently, flood inundation of the Nakkhu River, a major southern tributary of the Kathmandu river basin in Nepal. We used the CAESAR-Lisflood model to simulate flood inundation and sediment transport using a high-resolution digital elevation model, field-derived sediment grain size, and observed daily discharge data. To accurately replicate present field conditions by incorporating recently constructed embankments in a DEM that predates their construction, we employed a novel approach involving the creation and application of two distinct digital elevation models: a surface DEM and a bedrock DEM. The bedrock DEM, representing the subsurface layer, was used to effectively manage flow and sediment erosion beyond the embankment walls, ensuring more accurate simulation of the terrain and hydrodynamic interactions. The model was validated using field-observed data. The study presents outcomes for various flow scenarios, both operational and extreme, with and without sediment transport.

2. Study Area

2.1. The Nakkhu River

The Nakkhu River is located within the Bagmati basin in central Nepal, Kathmandu (Figures 2a and 2b). It initially flows westward from the south-east corner of the basin before turning northward until it joins the Bagmati River as one of the river's seven major tributaries (Figure 2b). It is 26 km long and has a watershed area of 58 km^2. The elevation of the basin varies from 1,200 m to 2,700 m above mean sea level. The Kathmandu region observes four distinct seasons: pre-monsoon (March–May), monsoon (June–September), post-monsoon (October–November), and winter (December–February). Summer temperatures average between 28 and 30 degrees Celsius, whereas winter temperatures can drop to 0 degrees Celsius (from December to January) (Aryal et al., 2008). Mean annual precipitation in the area is approximately 1,660 mm with a standard deviation of 243 mm, and roughly 80% of the rainfall occurs during the monsoon season (Shrestha et al., 2023). From the historical record obtained from the Tikabhairav hydrological station on the Nakkhu River (1963–1980) (Figure 2b), the annual mean flow of the river was approximately 1.1 m^3/s. In August, the average of the maximum monthly discharge reached its highest at 16.7 m^3/s, whilst in April, the average of the maximum monthly discharge was at its lowest, 0.26 m^3/s. Historically, the highest recorded instantaneous peak flood discharge of the river was 181 m^3/s on 24 August 1966. The highest recorded maximum monthly discharge was 104 m^3/s in August 1966.

2.2. Study Reach

2.2.1. Progressive Urbanization

Along the Nakkhu River, rapid urbanization has prompted the construction of river embankments, similar to other rivers in the Kathmandu valley (Figures 3a–3f). The Nakkhu River provides an excellent example of the impact of river embankments on sediment transport. Among all the tributaries of the Bagmati River, we observed that the anthropogenic impact on sediment mobility is likely to be higher in the Nakkhu River due to large-scale upstream sand and gravel mining activities. Embankments are planned for a 14 km reach of the river from the confluence with the Bagmati River to the Tikabhairav hydrological station upstream (blue star and square in Figure 2b, respectively). Construction began at the end of 2017 and is ongoing. A 6.5 km stretch of the river (black square outline in Figure 2b) was selected as the study reach because floodplain urban expansion is more pronounced in this region and the construction of embankments has mostly been completed in this region already.

Floodplain encroachment by expanding urbanization and river constriction by embankment construction along the Nakkhu River can be seen clearly through comparison of the satellite images in Google Earth taken at different times from 2003 to 2022 presented in Figures 3a–3f. The images are from the location at the downstream confluence where the Nakkhu River meets the Bagmati River. In the images, it can be seen that embankment construction had commenced by the end of 2017 (Figure 3e). Following embankment construction, a large

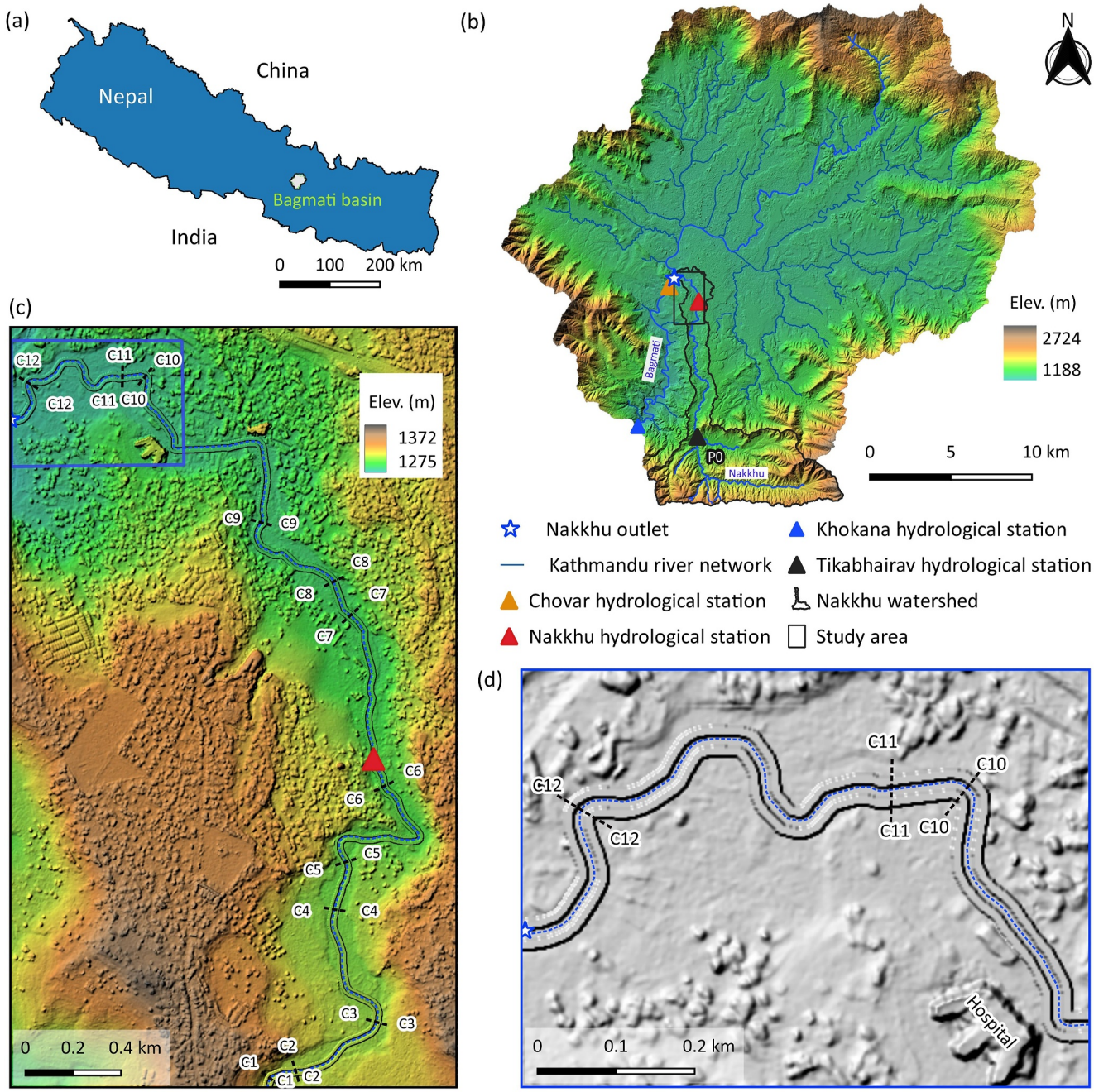

Figure 2. Overview of study area: (a) Location of study area. (b) River network within the Kathmandu basin, with the boundary of the Nakkhu watershed in the southeastern region indicated by a solid black line. The confluence of the Bagmati and Nakkhu rivers is denoted by a white star with a blue outline. The rectangle represents the study river reach. (c) Digital Elevation Model (DEM) depicting the studied river reach, indicating embankments and the river thalweg (marked by a dotted blue line). C1-C1 to C12-C12 are locations where field-measured river cross-sections and photographs were compared against simulated results for model validation. (d) Close-up downstream view of the study reach, highlighting embankments and the river thalweg, indicated by a dotted blue line.

number of buildings and apartments have been built and more are under construction in the floodplain, particularly on the left bank of the river near the confluence (Figure 3f).

2.2.2. Anthropogenic Activities

Rapid urbanization and increased human activities have caused significant changes in sediment supply to the Nakkhu River. Upstream sand and gravel mining, stone quarrying, and the construction of river corridors with

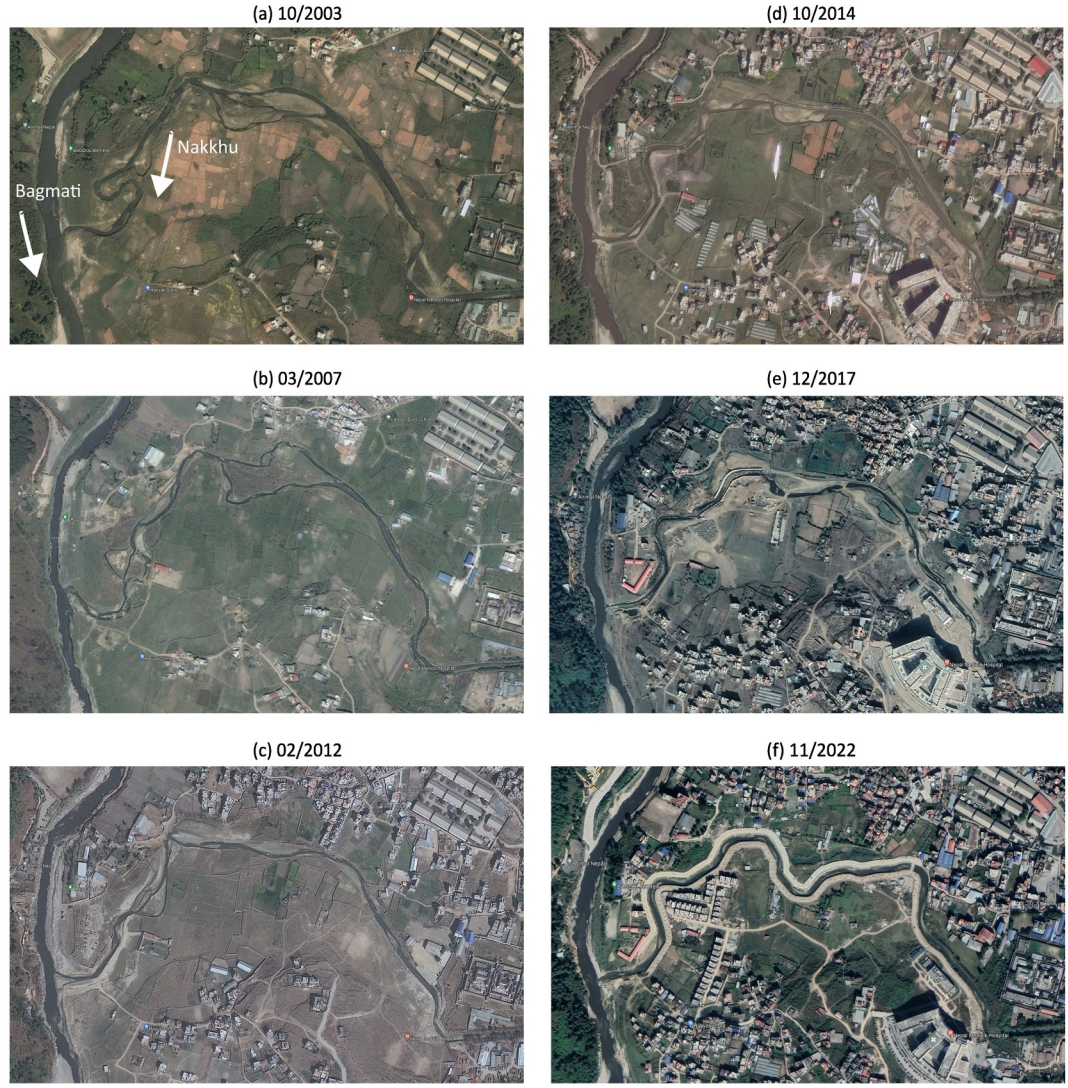

Figure 3. Satellite images in Google Earth taken at the same location at different times from (a–f) between 2003 and 2022 illustrate rapid urbanization and alternations in river course, influenced by both natural processes and human interventions. These images were taken near the confluence where the Nakkhu River meets the Bagmati River. Embankment construction commenced toward the end of 2017 and is substantially complete at the time of writing. A satellite image (10/2023) for the full length of the study area is provided in the Figure S1 of Supporting Information S1.

concrete and stone masonry embankments have further altered natural flow paths, modifying the conveyance capacity of river channels by sedimentation raising the river bed (Figure 4). Expansion of settlements along the river has exacerbated flood risk in the area.

3. Materials and Methods

3.1. Model Overview and Data Sources

3.1.1. CAESAR-Lisflood

We use a coupled hydrodynamic and landscape evolution model (LEM), CAESAR-Lisflood (Version 1.9j) (available at the website https://sourceforge.net/p/caesar-lisflood/wiki/Home/) (Coulthard et al., 2013) to simulate water and sediment discharges (using Wilcock and Crowe (2003) sediment transport) for a 6.5 km reach of the Nakkhu River upstream from the Nakkhu and Bagmati confluence (Figure 2c). The river width in the study area was about 30 m before embankment construction and about 13 m afterward. Given the reduced width of the river

Figure 4. Close-up view of study area with blue arrows showing the flow direction: (a) mining activities contribute sediment to the river, at nearby locations P0 see Figure 2b; (b) river constriction due to embankments and temporary settlements in the adjacent floodplain (photographed at cross-section C4-C4 location indicated in Figure 2c); (c) sediment mobility in the channel, with gravel bar formation evident in the inner bend and erosion in the outer bend at river meanders (photographed at cross-section C7-C7 location marked in Figure 2c); and (d) river encroachment due to urbanization and scouring observed at the right embankment (photograph captured at cross-section C10-C10 location indicated in Figure 2c).

after embankment construction, we utilized the highest available DEM resolution of 2 m. The 6.5 *km* reach length is suitable for the 2 m resolution DEM (1.53 million grids), fitting within the maximum grid number constraints of the CAESAR-Lisflood (C-L) model, which can accommodate up to 2 million grid cells (see the website https://sourceforge.net/p/caesar-lisflood/wiki/Instructions/). Key data inputs for the C-L model include a digital elevation model (DEM), hydraulic data, and sediment grain size distribution (GSD) data. In order to incorporate newly constructed embankments, the model required two layers of DEM (surface and bedrock DEMs), which were generated through DEM processing (see below in Section 3.2). The roads along both left and right embankments were also included, as shown in Figure 7. The majority of model parameters were selected following S. Thapa, Sinclair, Creed, Mudd, et al. (2024)'s study of the same river reach. The values of certain parameters, such as "Min Q for depth calc," "Courant number," and "Slope for edge cells" in the flow model section and other parameters that depend on the resolution of the DEM (refer to the model parameter description at the website https://sourceforge.net/p/caesar-lisflood/wiki) were updated from S. Thapa, Sinclair, Creed, Mudd, et al. (2024) for this study because of the use of a higher resolution DEM. Document S1 in Supporting Information S1 lists all model parameters used herein.

3.1.2. Digital Elevation Model (DEM)

The DEM was constructed from tri-stereo Pleiades satellite images obtained on 25 December 2019 and 13 January 2020. IDs of the images used to construct the DEM are provided in the Document S2 of Supporting Information S1. The panchromatic band (0.5 m resolution) was processed using rational polynomial coefficients (RPCs) in Agisoft Metashape v1.8.4 to create a 2 m resolution DEM.

3.1.3. Hydrology Input

Flow stage and discharge data were supplied by the Department of Hydrology and Meteorology (DHM), Nepal. The data were collected from Tikabhairav (1963–1980), Nakkhu (2018–2021), Chovar (1963–1980), and Khokana (1992–2020) stations (Figure 2). As per the DHM's hydrological analysis (refer to the website https://www.

dhm.gov.np/hydrology/hms), the water warning level at the Nakkhu hydrological station in Bungamati is set at 2.30 m, and the danger level is at 3.00 m.

We modeled four flood events: a historical 25-year return-period flood, equivalent to the design discharge for each embankment, as well as 50-year, 100-year, and 1000-year return-period flood forecasts obtained using the Generalized Logistic Model (Institute of Hydrology, 1999) using historical discharge data covering 26 years (1992–2017, inclusive). Due to the limited observed discharge data available, discharge time series for the Nakkhu River were generated using the drainage area ratio approach, which is widely used for ungauged rivers (Emerson et al., 2005; Marahatta et al., 2021; Yilmaz & Onoz, 2020). Details of the method are given by S. Thapa, Sinclair, Creed, Mudd, et al. (2024), who obtained a strong correlation (R-squared value of 0.717) between historically recorded floods in the Nakkhu River (Tikabhairav station) and corresponding floods in the Bagmati River (Chovar station) (S. Thapa, Sinclair, Creed, Mudd, et al., 2024). The historical maximum instantaneous discharge recorded at the Tikabhairav hydrological station on 24 August 1966, was 181 m^3/s. This is exceptionally high for the river, significantly higher than the forecasted 1000-year return period flood of 95 m^3/s at Tikabhairav. This event appears to be an outlier in the data record. The flood may have been caused by upstream damming and outburst flooding, as reported by the local community during our field work (November 2021). Due to lack of sediment flux and inundation data for the 1966 event, we do not consider this exceptionally high flood in our flood forecasting analysis. However, the scale of the 1966 event suggests that modeling higher return period flood scenarios is required for the Nakkhu River. Due to the limited discharge time series available, inflow hydrographs for the Nakkhu River were generated by downscaling the maximum recorded daily average hydrograph of July 2002 at Khokana hydrological station using the catchment area ratio approach. Details of the method are given by S. Thapa, Sinclair, Creed, Mudd, et al. (2024), who found a good correlation between historical recorded floods of the Nakkhu River at Tikabhairav station and corresponding floods of the Bagmati River at Chovar station (S. Thapa, Sinclair, Creed, Mudd, et al., 2024). A daily hydrograph was used as input for the model because recorded discharge data at higher resolution were not available at the time of the study.

To incorporate the effect of climate change on the 25-year design discharge of embankments, flood events with different return periods were considered, following S. Thapa, Sinclair, Creed, Mudd, et al. (2024). The forecast 100-year and 1000-year floods in the Nakkhu river (S. Thapa, Sinclair, Creed, Mudd, et al., 2024) have similar magnitudes to the median and the maximum mid-future (2046–2075) 25-year return period floods, respectively, derived by downscaling the Bagmati River's discharge as outlined by Shrestha et al. (2023). For the climate change projections, Shrestha et al. (2023) analyzed historical extreme rainfall patterns across the Bagmati basin using General Circulation Models. The terms “25-year,” “50-year,” “25-year median mid-future (25-year median MF),” and “25-year maximum mid-future (25-year max MF)” will be used hereafter to refer to the foregoing flood events.

The flood scenarios were used to conduct a sensitivity analysis of sediment transport (erosion and deposition) and inundation area with increasing discharge magnitude with and without sediment transport. The selection of discharge magnitudes was also informed by Zischg and Bermúdez (2020) who reported that Nepali rivers are particularly sensitive to changes in flood magnitudes within the 50-–100-year return period and that flood exposure increases sharply following overtopping of flood control structures when the design discharge is exceeded. It should be noted that Zischg and Bermúdez (2020)'s findings were based on a global approach which did not account for the impact of sediment transport.

3.1.4. Sediment Data

The models were run in sediment re-circulation mode due to insufficient observed data on sediment flux entering from upstream sources. To verify the reliability of the results generated by the model in sediment re-circulation mode, the predicted sediment outflow was compared with that estimated using suspended sediment measurements (obtained June–October 2022) from the Nakkhu River. Data on suspended sediment concentrations in the Bagmati River at the Khokana gauging station were obtained from the DHM, Nepal. The data comprised daily measurements taken during the monsoon season and biweekly data during the pre- and post-monsoon periods from 2003 to 2020, except for a few years with missing data records. We also sampled and measured the suspended sediment concentrations in the Nakkhu River at Tikabhairav station biweekly during a monsoon in 2022 (July– October) (see Figure S2 in Supporting Information S1). The suspended sediment concentration data were used to estimate the suspended sediment load, which was used in model calibration. The estimated suspended load was also used to approximate the bedload of the river using a rough approximation of 35% of the total sediment

load as mentioned in the previous research in Himalayan Rivers (Pratt-Sitaula et al., 2007; S. Thapa, Sinclair, Creed, Mudd, et al., 2024; Turowski et al., 2010). To determine the grain size distribution of bedload on gravel bars, we used a method of sieving and weighing proposed by Attal and Lavé (2006), Dingle et al. (2020) and S. Thapa et al. (2022); S. Thapa, Sinclair, Creed, Mudd, et al. (2024). We sampled grain size distributions at six different locations and computed nine average bin classes for use in the numerical model. The field-derived average sediment grain size distribution data are provided in the Document S1 of Supporting Information S1. A full description of the sediment data collection and analysis is given by S. Thapa, Sinclair, Creed, Mudd, et al. (2024).

3.1.5. Field Observations; Channel Profile and Backwater Effect

Annually, after each monsoon in November (2020–2022), field measurements were taken of the relative change in river channel geometry, bed slope, and sediment erosion and deposition along the embankments with reference to the crest of the embankments using a laser range finder and survey staff. These data were used to validate the numerical model (Figures 9–15). High water level marks on the embankment walls of the Nakkhu River, and fine sediment deposits at the confluence of the Nakkhu and Bagmati rivers were also recorded during the field visits. These had been caused by a backwater effect at the confluence of the Bagmati and Nakkhu rivers during monsoon flood events. We used this information to calibrate the downstream slope parameter of the model, comparing simulated and observed downstream water levels.

3.2. Hydro-Conditioning and DEM Processing

Most landscape evolution models for natural river systems require a spin-up period for the model to become dynamically stable (Feeney et al., 2020; S. Thapa, Sinclair, Creed, Mudd, et al., 2024). For example, CAESAR-Lisflood may produce extremely high sediment transport rates during the early stage of a simulation as a result of initial surface roughness smoothing in the DEM and uniformity of sediment grain size distribution across the catchment (Feeney et al., 2020; S. Thapa, Sinclair, Creed, Mudd, et al., 2024). In our study, the insertion of embankments on both sides of the channel and the extraction of riverbed material through dredging to fill the embankments significantly transformed the river channel. In some places, the embankments were constructed by shifting the existing river thalweg horizontally by up to 130 m. Consequently, the initial condition of the embanked river more closely resembled an artificial canal. To replicate this initial condition, instead of running the model spin-up process required for a natural river, DEM pre-processing was carried out, involving channel smoothing and the addition of embankments to the DEM (Figure 5).

DEM smoothing is essential for stabilizing landscape evolution models, but it can obscure critical topographical features like crests and troughs (Figure 6), impacting the model's ability to replicate real-world conditions accurately (Shiono et al., 2009). While smoothing reduces noise and eliminates minor inaccuracies that could destabilize simulations, it can also oversimplify the terrain, leading to less precise predictions of water flow, sediment transport, and flood risk (Shiono et al., 2009). The challenge lies in balancing noise reduction with the preservation of key geomorphological details. In our study, DEM smoothing was necessary to accurately represent the modified, embanked river channel, despite some loss of natural features. This approach aimed to improve simulation reliability while maintaining enough detail to capture essential features of newly constructed embankments formed by dredging riverbed material, thereby enhancing the overall accuracy of flood risk predictions in our case study.

During DEM processing, various methodologies were tested. First, the r. carve function - GRASS in QGIS (osgeo.org) (refer to the website https://grass.osgeo.org/grass83/manuals/r.carve.html) removed pools and troughs from the original riverbed, resulting in a smoothed channel. However, the resulting elevation was incorrect and several meters below the present river bed level. Attempts were also made using HEC-RAS Mapper (available at the website https://www.hec.usace.army.mil/confluence/rasdocs/rmum/latest), but manual digitization was required and found to be inefficient for long river reaches. Consequently, a semi-automatic hydro-conditioning method in R (programming language) was adopted, which involved identifying and removing the erroneous spikes and valleys to generate a smoother channel (see Figure 6). This method uses functionalities of rgrass7 package in R and produces a post-hydro conditioning profile that minimizes the total squared error of pre- and post-hydro conditioning profiles. In this approach, we used the "despike" smoothing function available in the rgrass7 package in R to control the gap distance along the river thalweg and remove spikes. Several gap distances

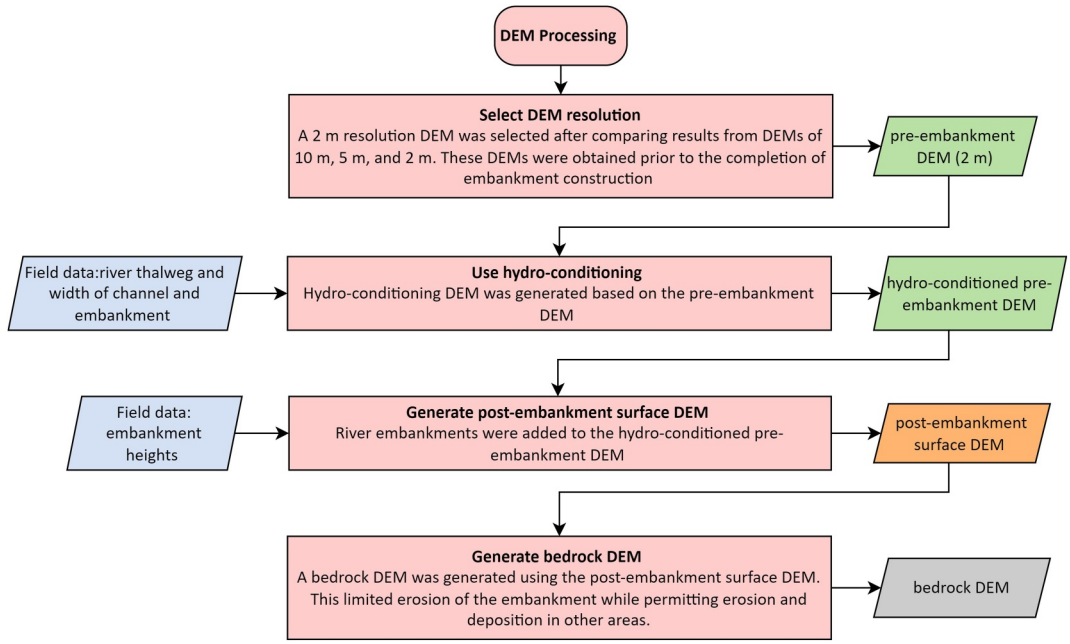

Figure 5. Flow chart showing DEM processing steps to adopt newly constructed embankments.

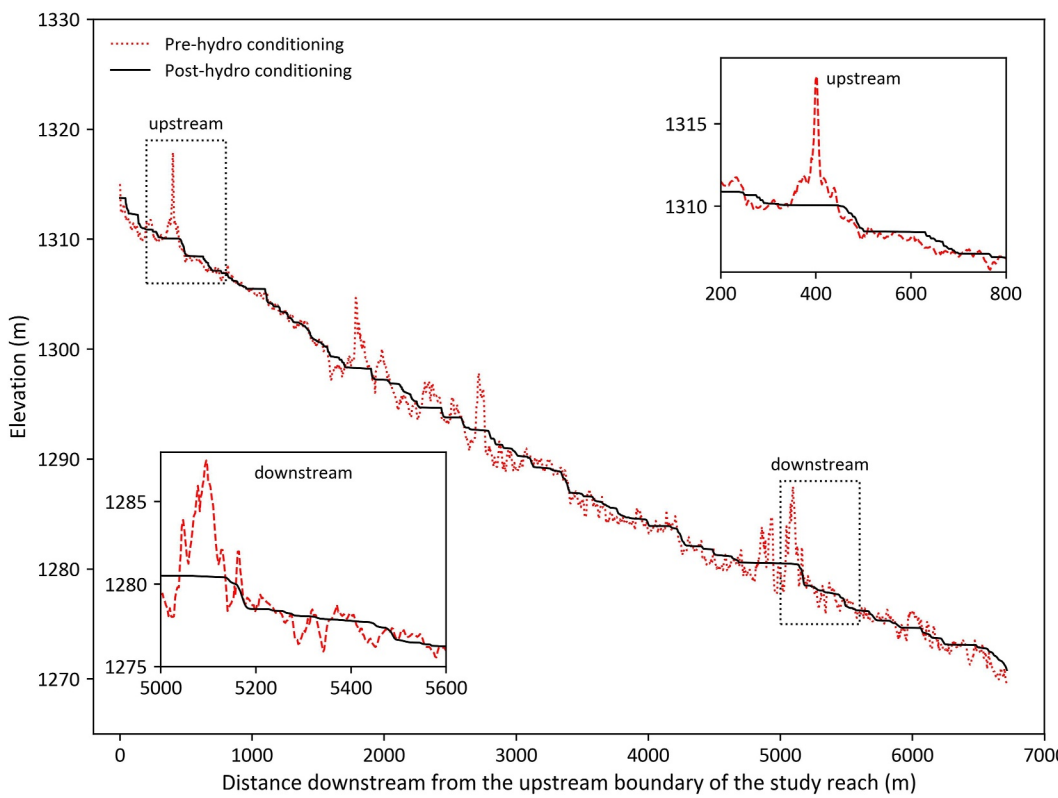

Figure 6. Longitudinal profiles of the river thalweg before and after hydro-conditioning whereby the crests and troughs of the original profile were averaged to produce a smoothed channel. The same river smoothing algorithm was used to produce smoothed DEM with uniform embankments on both sides of the river channel (Figure 7).

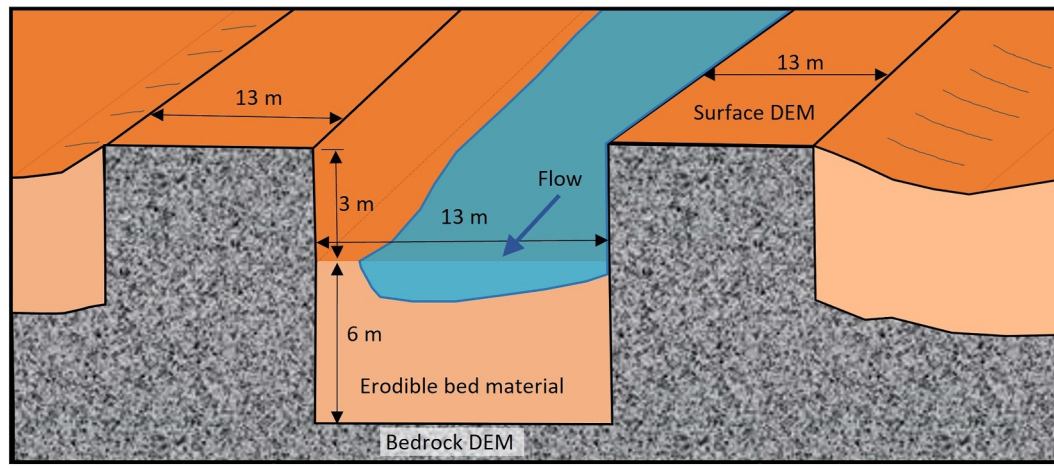

Figure 7. Sketch showing surface DEM (dark orange) and bedrock DEM (gray) incorporating newly constructed embankments. There is a 6 m thick erodible layer (light orange), except at the top of both embankments, which replicates the field-observed side roads each of width of 13 m on both sides. The newly constructed embankment height and channel width were 3 m and 13 m, respectively.

were tested, with 200 m found sufficient to minimize the error between pre- and post-hydro conditioning profiles. The method involved buffering the river thalweg to form a channel boundary polygon and the applying despiking techniques to smooth the river channel according to gap distance. The resulting smoothed channel within the channel boundary polygon was then embedded in the original DEM to generate a new DEM with a smoothed river channel.

Next, we introduced two embankments along both sides of the river channel, using surveyed embankment geometry in the raster calculator tool available in QGIS, as depicted in Figure 7. Although embankment construction began in late 2017, it was not entirely captured in our DEM. During the construction of the 3 m high, 13 m wide embankments, the river channel was constricted to a width of 13 m. Roads were placed on top of the left and right embankments. Constructed from dredged riverbed material, these side roads altered the appearance of the river channel, as portrayed in Figure 7. Within the numerical model we define the embankments as bedrock DEM to limit sediment erosion. For this reason, we used two DEMs (Figure 7): one representing the initial top surface of the terrain; the other a subsurface bedrock DEM representing the embankment and underlying bedrock layer depth. The depth between these two layers is composed of erodible material, which has the same grain size distribution as the river sediment.

3.3. Model Calibration

We calibrated the model for Manning roughness and downstream slope parameters. To minimize uncertainty introduced by these parameters, we initially took reference values based on previous research conducted by S. Thapa, Sinclair, Creed, Mudd, et al. (2024), who performed a model parameter sensitivity analysis for the same river. However, S. Thapa, Sinclair, Creed, Mudd, et al. (2024)'s study did not account for the presence of embankments. To address the sensitivity of Manning's n for cases involving embankments, we tested three uniformly distributed Manning roughness values of 0.03, 0.04 and 0.05 s.m$^{-1/3}$ (i.e., 0.04 $\pm$ 0.01 s.m$^{-1/3}$, or 25% variation) for the 25-year maximum mid-future flood event. Our results exhibited insignificant differences (less than 3%) in the predicted water outflow discharges. For sediment outfluxes, we computed the sediment concentration from a simulated suspended sediment outflow for each case; the values were found to be 1,556, 1,078, and 3,321 ppm for Manning coefficients of 0.03, 0.04, and 0.05 s.m$^{-1/3}$ (see Figure S3 in Supporting Information S1). By comparing the simulated sediment concentration against the maximum field-measured sediment concentration of 700 ppm during the peak monsoon flood of June 2022 (see Figure S2 in Supporting Information S1), we selected a Manning coefficient n of 0.04 s.m$^{-1/3}$, which produced sediment outflux close to the observed value.

Observed high water level marks on the embankment walls of the Nakkhu River, and fine sediment deposits at the confluence of the Nakkhu and Bagmati rivers were used to calibrate the downstream slope parameter of the

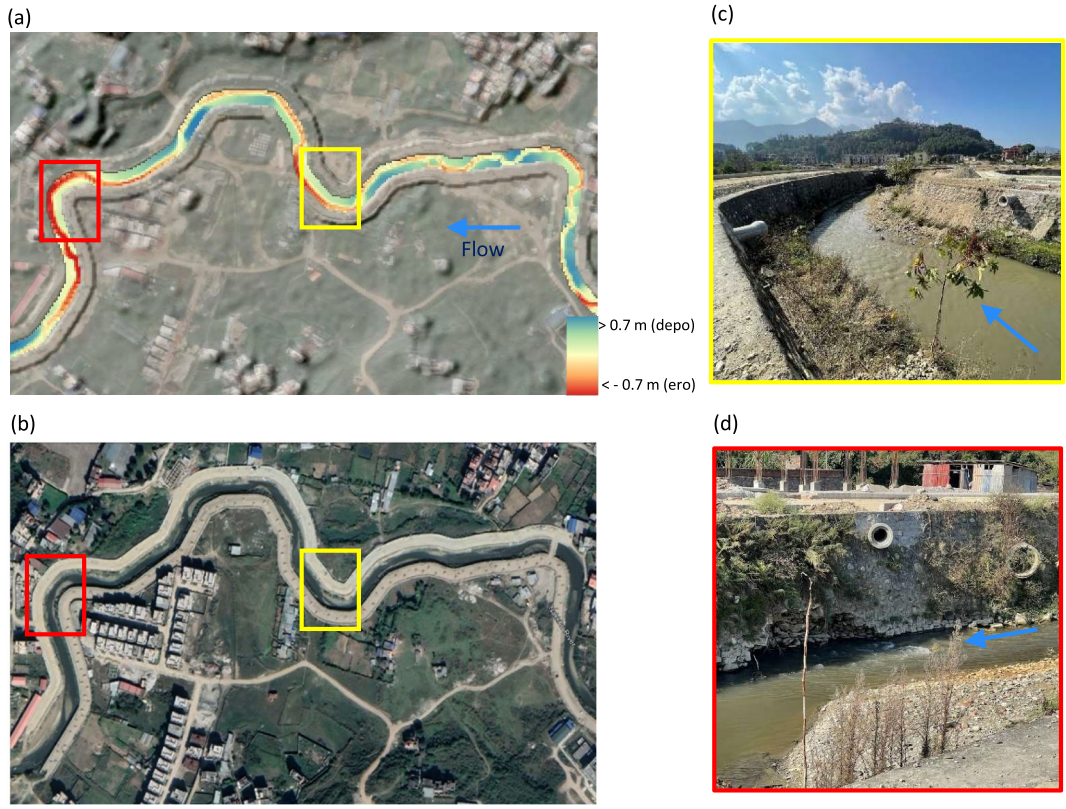

Figure 8. Comparison between simulated and field-observed sediment erosion and deposition in the Nakkhu River near the river confluence with the Bagmati River, including a satellite image from Google Earth: (a) overlay of simulated erosion and deposition map on satellite image; (b) observed erosion and deposition visible in the satellite image taken on 10 November 2022; and (c–d) observed erosion (~1 m) and deposition (~0.5 m) within the channel at the locations marked by red and yellow rectangles in images (a) and (b) (also photographed on 10 November 2022).

model. From the observations, we believe that the higher water stage of the Bagmati River affects the flow of the Nakkhu, leading to an increase in water level in the Nakkhu during extreme flood events. Comparing the results of a sensitivity analysis with the observed data, we found that the simulated inundation at the confluence was highly sensitive to the value of the downstream slope parameter used in the C-L model (0.01 and 0.001). It was found that a downstream slope of 0.001 provided the best representation of the backwater effect caused by the Bagmati River.

3.4. Model Validation Against Observed Erosion and Deposition

The model was validated by comparing simulated erosion and deposition, computed from the DEMs of difference (DoD), against field-measured in-channel erosion and deposition depths and patterns obtained approximately 3 years after embankment construction. The model simulation for validation used a daily discharge of 2.4 m^3/s that is approximately equal to the average monsoon discharge observed between 2017 and 2020 in the 2–3 year period between the embankment construction and our fieldwork. Figure 8 shows that the predicted erosion and deposition maps (Figure 8a) exhibit good qualitative agreement compared to a satellite image taken from Google Earth on 10 November 2022 (Figure 8b) and field-observed erosion and deposition patterns (Figures 8c and 8d) along the embankment of the Nakkhu River on 10 November 2022 (up to ± 1.5 m).

Field-measured in-channel erosion and deposition depths at 12 river cross-sections at different locations (Figure 2c) were compared with their simulated counterparts (see Figure 9). Positive values indicate deposition (blue dots) and negative values indicate erosion (red dots). There are two point locations (gray dots) where minor erosion was simulated but minor deposition was observed in the field. The comparison reveals a slight underestimation of simulated deposition depths and a slight overestimation of erosion depths. At several locations, field-observed embankment undercutting, indicated in Figure 8d, was not completely captured in the simulated

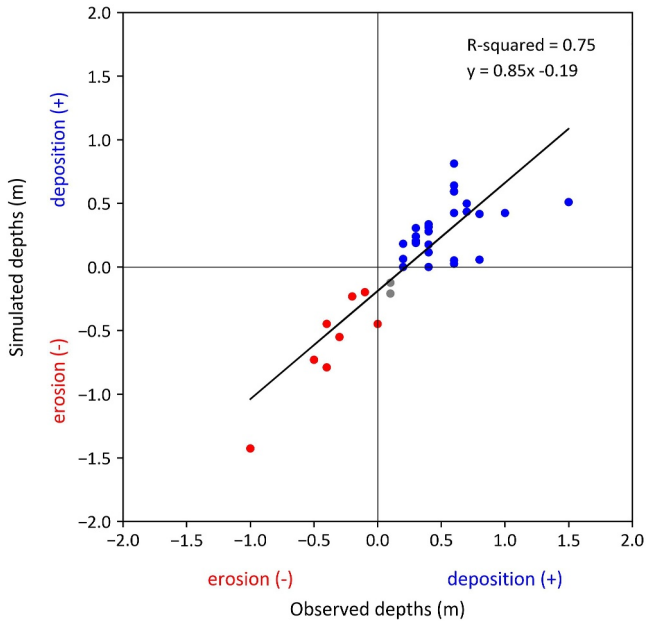

Figure 9. Observed versus simulated sedimentation depth data used to validate the numerical model.

DEMs of difference. This was because the embankment was assumed to be bedrock in the model and erosion underneath was not permitted due to a model limitation. Nonetheless, satisfactory agreement can be seen between the observed and simulated erosion and deposition depths, with an R^2-value of 0.75 (Figure 9) and a root-mean-square error (RMSE) of 0.334 m. Comparison between simulated and observed erosion and deposition at measured locations is also depicted in the cross-section profiles in Figures 14 and 15. The largest error in erosion occurs at the upstream cross-section C1-C1 (Figure 2), where the measured erosion of 1 m is less than the simulated erosion of approximately 1.4 m. Conversely, the largest difference in deposition occurs at the downstream cross-section C7-C7 (Figure 2), where the measured deposition of 1.5 m exceeds the simulated deposition of about 0.5 m. These errors are most likely due to the model being run in sediment recirculation mode. The predictions of higher erosion upstream and insufficient deposition downstream compared to field measurements suggest the model exhibits sediment supply limited characteristics due to the absence of upstream sediment inputs.

3.5. Model Scenarios

After model validation, eight model scenarios (S1–S8) were run to simulate different flood inundation and sediment transport cases using a high-resolution DEM, an average field-derived sediment grain size distribution from sieve analysis, and forecast flood events based on daily discharge obtained from the DHM. The eight simulations (S1–S8) were run using the post-embankment surface DEM and bedrock DEM. Additionally, four model scenarios (S9–S12) were run for a priori conditions to study the impact of newly constructed embankments on sediment transport and flooding (as detailed in Table 1).

4. Results

4.1. Flood Inundation and DEMs of Difference

Table 2 summarizes the flood inundation area and sediment (erosion/deposition) volume for all model scenarios (S1–S12). Among the first eight post-embankment model cases (Table 1), the first three scenarios without sediment transport (i.e., S1 to S3) have a similar flood inundation area of less than 0.01 ha, and the second three scenarios with sediment transport (i.e., S5–S7) have similar flood inundation of less than 1 ha and sediment

Table 1
Simulated Model Scenarios

Model scenario	Flood return period	Sediment input	Embankments
S1	25-year	No	Yes (after embankments)
S2	50-year	No	Yes
S3	100-year (25-year median mid-future)	No	Yes
S4	1000-year (25-year maximum mid-future)	No	Yes
S5	25-year	Yes	Yes
S6	50-year	Yes	Yes
S7	100-year (25-year median mid-future)	Yes	Yes
S8	1000-year (25-year maximum mid-future)	Yes	Yes
S9	25-year	Yes	No (before embankments)
S10	50-year	Yes	No
S11	100-year (25-year median mid-future)	Yes	No
S12	1000-year (25-year maximum mid-future)	Yes	No

Table 2
Summary of Simulated Inundation Area and Volumetric Change of Sediment Erosion and Deposition for the Different Flood and Sediment Scenarios (S1–S12)

Model scenario	Flood discharge (m^3/s)	Inundation area (m^2)	Sediment erosion volume (m^3)	Sediment deposition volume (m^3)
S1 (25-year, no sedi)	42.23	0.00		
S2 (50-year, no sedi)	49.77	624.71		
S3 (25-year median MF, no sedi)	58.22	748.71		
S4 (25-year max MF, no sedi)	95.07	50,520.72		
S5 (25-year, with sedi)	42.23	2,929.49	23,677.74	23,375.64
S6 (50-year, with sedi)	49.77	3,552.70	24,231.47	23,887.84
S7 (25-year median MF, with sedi)	58.22	8,048.71	25,108.64	24,749.45
S8 (25-year max MF, with sedi)	95.07	243,512.72	40,793.36	40,609.71
S9 (25-year, with sedi)	42.23	224,556.00	59,564.03	59,399.05
S10 (50-year, with sedi)	49.77	243,376.00	24,231.47	23,887.84
S11 (25-year median MF, with sedi)	58.22	251,992.00	57,527.55	57,260.61
S12 (25-year max MF, with sedi)	95.07	288,116.00	103,785.03	103,302.22

erosion/deposition volume (Table 2). We therefore selected S1 as a representative scenario of S1–S3, and S5 as representative of the S5–S7 scenarios. As a result, the major flood scenarios shown in the following figures are S1, S4, S5, and S8. Here S1 and S5 represent a 25-year flood event without and with sediment transport, respectively. S5 and S8 represent a 25-year maximum mid-future (25-year max MF) flood event without and with sediment, respectively. A comparison of flood inundation for pre- and post-embankment cases (S1–S12) for 25-year and 25-year max mid-future flood is presented in Figure S4 of Supporting Information S1. The inundation area predictions listed in Table 2 indicate that inundation would reduce after embankment construction. This is due to the reduction in channel width, and flow control preventing inundation from spreading (Figure S4 in Supporting Information S1). The reduction in flooding after the construction of embankments is up to 99% (from 22.5 to 0.3 ha) for a 25-year flood of 42 m^3/s (equal to the embankment design discharge), and is about 15% (from 28.8 to 24.3 ha) for a 25-year maximum mid-future flood of 95 m^3/s.

We now consider the downstream region of the Nakkhu River, near the confluence with the Bagmati (Figure 10). In cases where sediment transport is not incorporated that is, scenarios S1–S4, the simulated flood inundation depths indicate that the embankments can contain a discharge equivalent to a 25-year flood event, S1 (Figure 10a), and up to a 25-year median mid-future flood event; however, about 1 km of the 6.5 km studied reach experiences inundation for a 25-year maximum mid-future flood event, S4 (Figures 10b and 11a). The inundation is caused by embankment overtopping and backwater flow at a sharp bend in the river channel where the velocity slows.

When sediment transport is included in the simulations, that is, scenarios S5–S8, instances of overtopping and flooding increase compared to the no-sediment cases, especially in areas where embankments align with meandering channel courses (e.g., see the inundation for a 25-year maximum mid-future flood event depicted in Figures 10b and 10d near the confluence and Figures 11a and 11b for the full reach). This inundation is particularly pronounced for a 25-year median mid-future magnitude flood event or higher, where increased overtopping is observed downstream (Table 2). The DEM of difference maps (Figures 10e and 10f) indicate that sediment mobility significantly influences alterations in river morphology due to erosion and deposition, causing considerable fluctuations in the channel's capacity to carry water subsequent to embankment construction. Figures 10e and 10f show erosive channels are cutting across the floodplain to bypass large meanders in the embanked channel. These acts like “chutes” across the floodplain, as generally observed in meandering channel systems. The simulated DEM of difference maps for all scenarios with sediment transport S5 to S8 indicate that erosion, greater than 1 *m* at certain locations, occurs in the straight reach of the channel and at outer bends of the river meanders, with deposition and formation of gravel bars at inner bends (Figures 10e and 10f).

The simulated flood inundation areas obtained for scenarios S1–S4 (Table 2) demonstrate the effectiveness of embankments at managing an expected design discharge equivalent to a 25-year flood when sediment mobility is neglected. In scenarios representing 50-year flood and 25-year median mid-future flood events in the absence of sediment transport, minimal flooding occurs, highlighting the resilience of the embankments. For lower

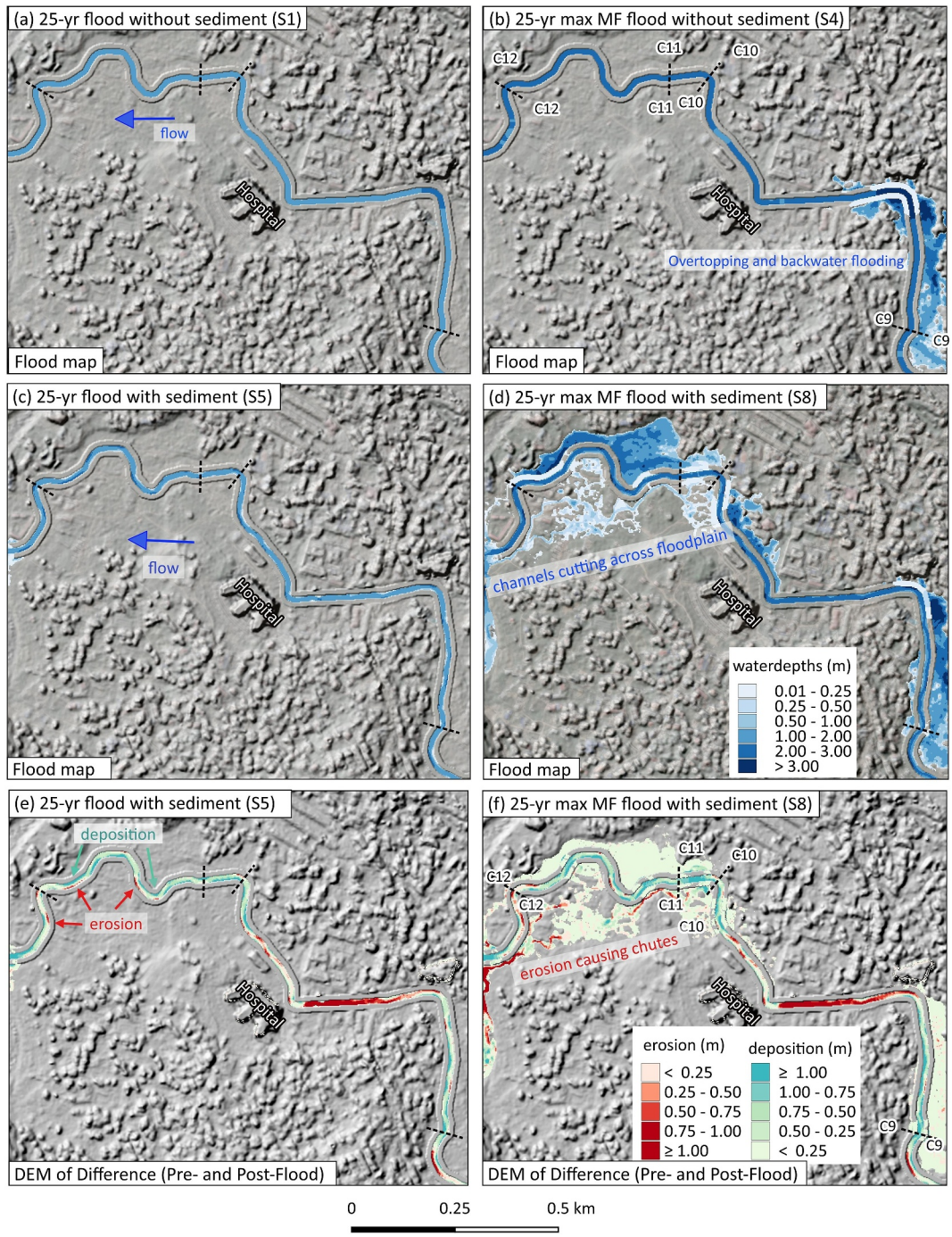

Figure 10. Post-embankment flood maps and DEM of difference maps: (a) 25-year flood map and (b) 25-year maximum mid-future flood map excluding sediment transport effects; (c) 25-year flood map and (d) 25-year maximum mid-future flood map incorporating average observed sediment transport effects; and (e) 25-year flood- and (f) 25-year maximum mid-future flood-driven erosion and deposition maps.

magnitude flood events, inclusion of sediment transport in the model increases flood inundation by a factor of 5–10, though it should be noted that the overall inundation area remains minimal (< 1 ha). For the 25-year maximum mid-future flood event, the inclusion of sediment transport increases the inundation area significantly from 5.1 to 24.4 ha. Although the increase in inundation area appears relatively small, the population density of the Kathmandu city area is approximately 20,288 persons per km^2 (or per 100 ha) and growing rapidly; therefore, even a

10.1029/2024WR037742

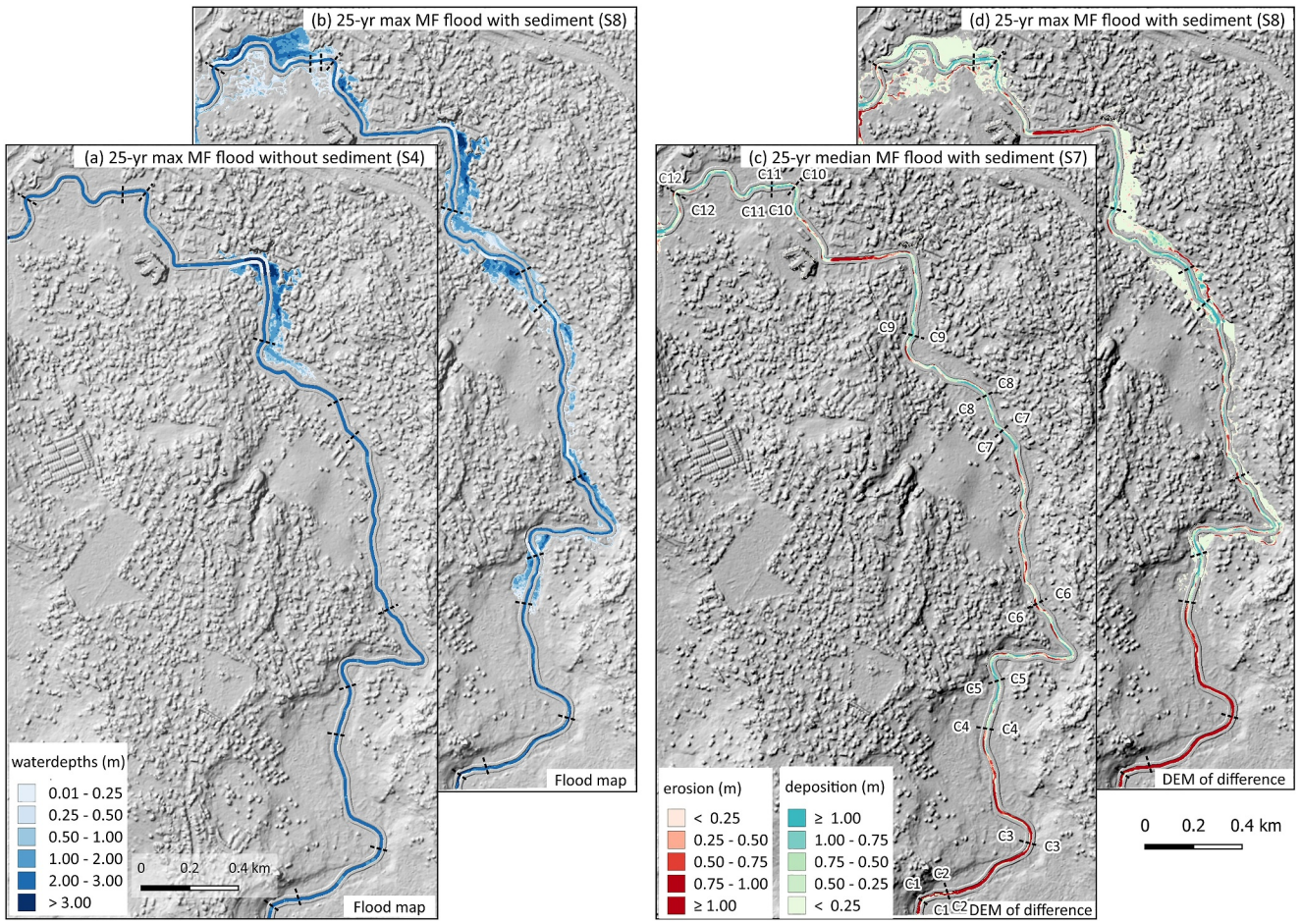

Figure 11. Post-embankment flood maps and DEM of difference maps for the whole study reach: (a) 25-year maximum mid-future (25-year max MF) flood map without sediment; (b) 25-year maximum mid-future flood map with sediment; (c) 25-year median mid-future (25-year median MF) flood-driven sediment erosion and deposition map; and (d) 25-year maximum mid-future flood-driven erosion and deposition map.

small inundation < 1 km^2 could affect thousands of people. Sediment transport does not result in a significant increase in inundation for lower magnitude floods. However the inclusion of sediment transport could alter embankment stability by sediment erosion (and potential undercutting) which is observed in all embanked channel scenarios S5–S8 (see river cross-section in Figures 14 and 15 and Figure S5 in Supporting Information S1).

Table 2 shows that embankments designed for a 25-year flood in the Nakkhu River are unlikely to expose a population to floods occurring at a return period lower than the 25-year return period flood in the absence of sediment transport. However, when sediment transport is accounted for, flood inundation increases rapidly from the 25-year median mid-future (25-year median MF) to the 25-year maximum mid-future (25-year max MF) flood events. Notably, the inclusion of sediment significantly amplifies flood inundation by five times from 5.05 to 24.35 ha for a higher flood scenario (S8 in comparison to S4, in Table 2). Given that the highest flood event recorded in the Nakkhu in recent history had a magnitude almost double the 25-year maximum mid-future discharge, this is an important consideration for future flood management in the region.

4.2. Sediment Transport and Its Impact on Channel Morphology

4.2.1. Sediment Transport

Table 2 reveals that the presence of river embankments reduces flood inundation significantly up to 99% for a flood equal to the embankment design discharge and only 15% for an extreme flood of 95 m^3/s (a 25-year

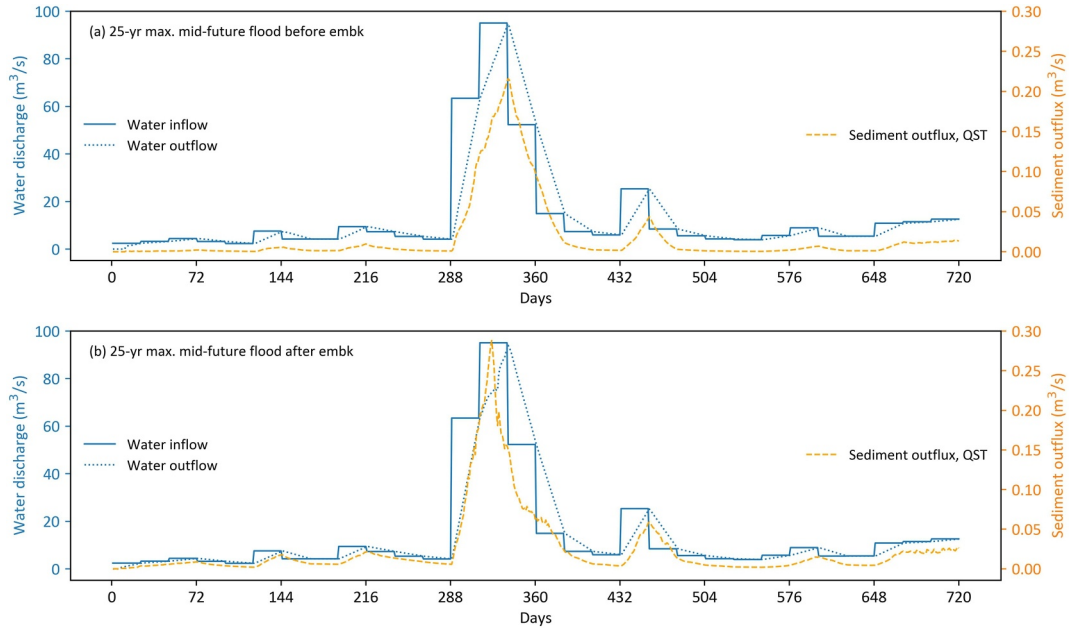

Figure 12. Computed water-sediment flows (hourly mean) in the Nakkhu River: (a) before; and (b) after embankment construction. The left hand ordinate shows the water discharge, and the right hand ordinate shows total sediment throughput corresponding to a 25-year maximum mid-future flood events.

maximum mid-future flood). Moreover, we find that embankment construction increases the sediment transport rate by about 32% (e.g., 0.22 m^3/s to 0.29 m^3/s corresponding to a flood of 95 m^3/s) (Figure 12).

The simulated sediment volumetric change (erosion and deposition) from the DEM of difference is similar for the lowest magnitude flood scenarios S5, S6, and S7, with a marginal increase in morphological change observed as discharge increases. For the 25-year maximum mid-future flood case S8, the total sediment erosion/deposition volume is approximately double that of the other cases (Table 2 and Figures 11c and 11d). The higher erosion and deposition of sediment in flood scenario S8 is primarily attributed to the sedimentation processes that occurs in the floodplain after overtopping, although there is also a minor increase in in-channel erosion and deposition when compared to scenarios S5–S7 (Figures 11c and 11d).

In the context of extreme flood events, intense bedload transport plays a crucial role in driving morphology changes in the embanked river channel. In the model, the finest sediment grain size bin (diameter, $d = 0.0375$ mm) is considered the suspended sediment load, and the other eight bins are the bedload. Our simulation shows around 35% bedload contribution to total sediment load corresponding to the flood peak up to a 25-year median mid-future; whereas for the 25-year maximum mid-future flood peak, there is a significant increase in bedload transport, contributing approximately from 60% to 90% to total sediment transport during the peak flood event in the embanked river channel (Figure 13 and Figures S6–S7 in Supporting Information S1).

In this study, we present simulated results at high temporal resolution (hourly). Initially, we exported outflow hydrographs, inundation (water depths), and sediment erosion/deposition maps (via DEM of difference) at both daily and hourly intervals. Upon comparing these outputs, we found that the daily interval results tended to underestimate the impact of maximum instantaneous discharges, which may last only a few hours but are sufficient to cause significant loss of life and property during extreme floods. Temporal resolution in simulations therefore plays a crucial role in the accuracy of flood predictions. Reliance on daily mean discharge can obscure the effects of peak instantaneous discharges, especially for rivers where floods are brief but intense. By contrast, hydrographs generated at hourly intervals successfully capture these peak discharges, providing a more accurate depiction of flood dynamics. This approach also illustrates the benefits of analyzing floods based on peak flood magnitudes rather than solely on daily mean discharge data. Therefore, in this study, we exported the model output at hourly intervals to improve the accuracy of flood risk assessments by capturing detailed flood dynamics during maximum instantaneous discharge events.

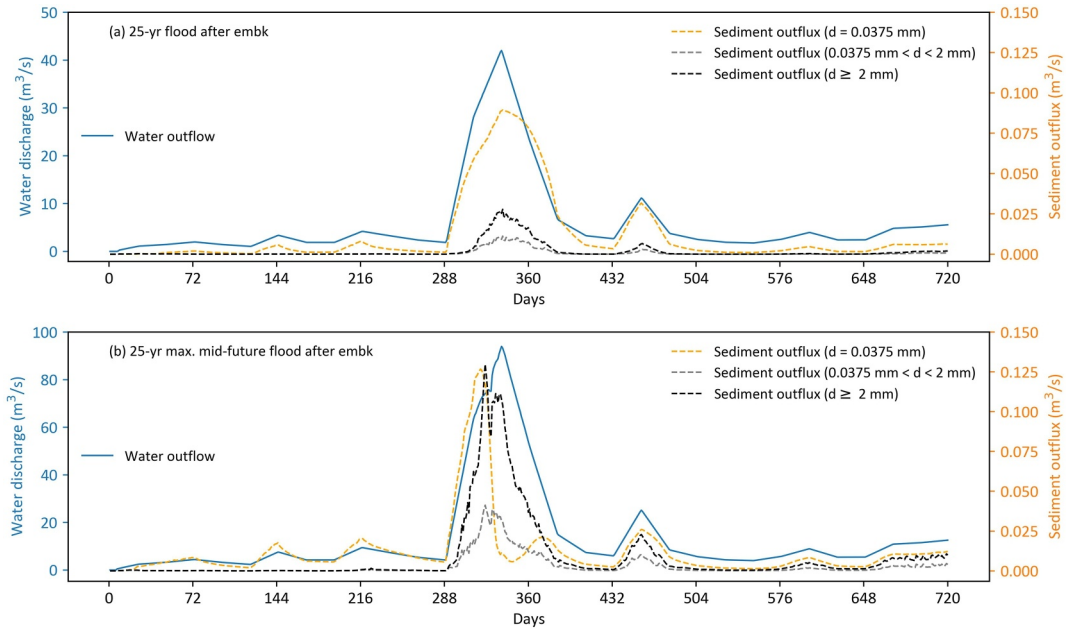

Figure 13. Computed water-sediment flows (hourly mean) in the Nakkhu River after embankment construction. The left hand ordinate shows the water discharge outflow, and the right hand ordinate shows sediment throughput corresponding variations with outflow river discharge for the three classes of GSDs; finest sediment grain size bin ($d = 0.0375$ mm) in suspension, and other bedload classes as median grain bins (0.0375 mm $< d <$ 2 mm) and coarser grain bins ($d \geq 2$ mm) for: (a) 25-year flood; and (b) 25-year maximum mid-future flood.

4.2.2. Impact of Sediment Transport on Channel Geometry

The impact of sediment transport on river bed morphology was evaluated by considering in-channel erosion and deposition estimated using the DEM of difference of pre- and post-flood DEMs for each scenario. Figures 14 and 15 present cross-section profiles from upstream to downstream (C1-C12) (see Figures S8 and S9 in Supporting Information S1 for other cross-sections) obtained from the DEM of difference for the model validation case (top row) and two model scenarios: the 25-year flood event S5 (middle row) and the 25-year maximum mid-future flood event S8 (bottom row). Observed erosion and deposition depths are displayed as black dots alongside the validation case displayed as black dots. Erosion is shown in red and deposition in blue. Both simulated and observed cross-sections at the upstream reach (C1-C3) (Figure 14) have relatively higher sediment erosion compared to the other cross-sections (C4-C12) (Figure 15 and Figures S8 and S9 in Supporting Information S1) downstream. Changes in channel geometry can also alter the riverbed slope, leading to significant variations in sediment transport. An increased slope and narrower channel width upstream can result in accelerated erosion and higher sediment transport, while downstream, the reduced slope and flatter terrain may lead to substantial sediment deposition. These mechanisms create a pronounced shift from erosion to deposition along the course of a river.

4.3. Post-Embankment Conveyance Capacity Variations of the Channel

We now assess the conveyance capacity of the Nakkhu River using two sets of channel geometry data. The conveyance capacity is the bankful discharge that can be transported by the considered river section. The first data set, representing the initial design channel capacity just after embankments have been constructed on both river banks (herein referred to as the design channel capacity) was compared with the second data set obtained from field measurements conducted 2–3 years after embankment construction (10 November 2022) across 12 different river sections (Figure 16). Channel capacity (discharge) was calculated using the Manning formula. In both cases, the calculated channel capacity surpasses the 25-year median mid-future flood. The design channel capacity (black solid line in Figure 16) is capable of safely accommodating the 25-year maximum mid-future flood event at most cross-sections. However, since the construction of the embankments, it can be seen that the channel capacity has reduced due to sedimentation within the channel at all cross-sections (green solid line in Figure 16), leading to

10.1029/2024WR037742

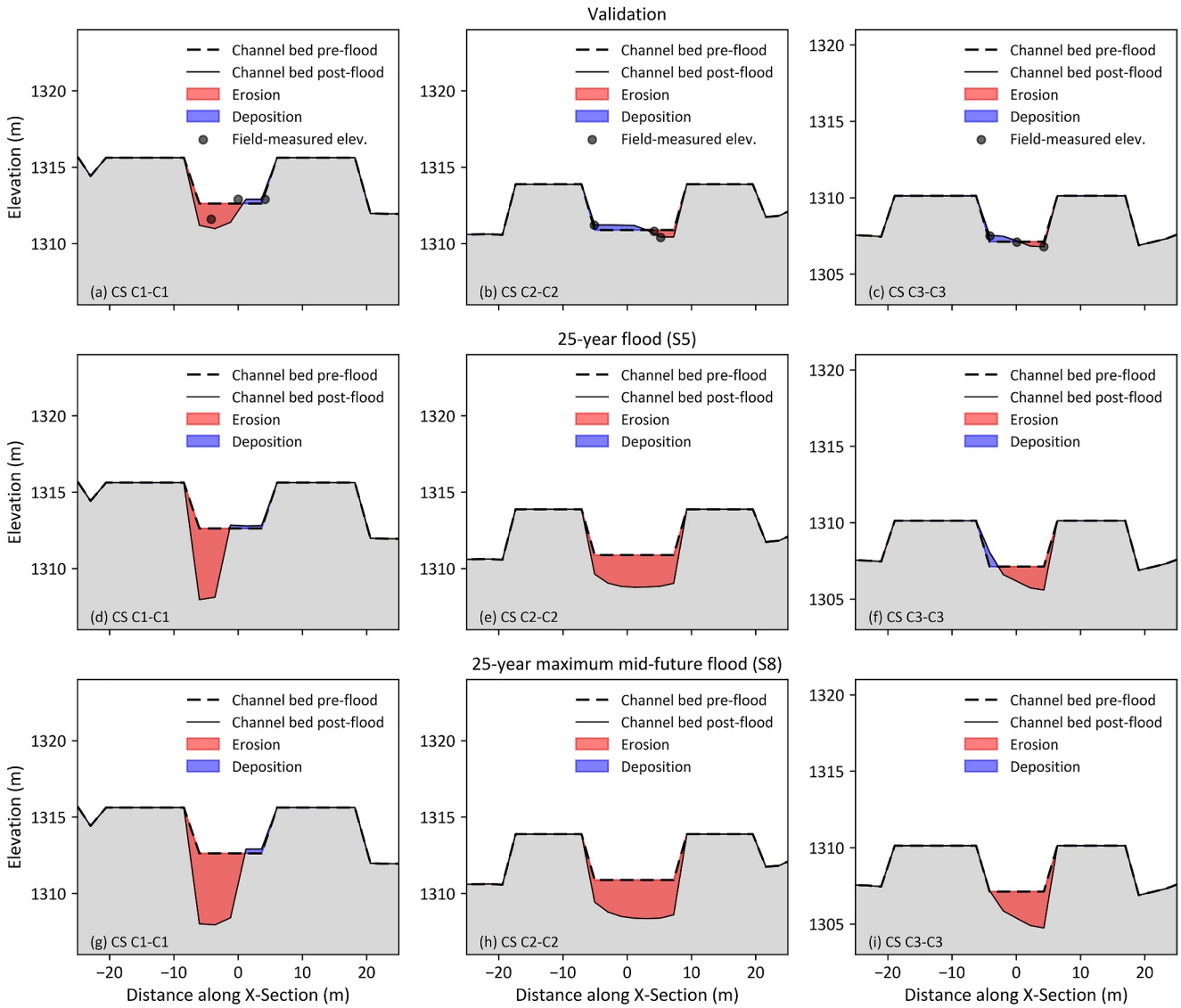

Figure 14. Simulated river cross-section profiles at sections C1 to C3 (upstream reach, Figure 2c) for validation case (top row), 25-year (middle row), and 25-year maximum mid-future (bottom row) return period flood events. Black dots represent observed erosion and deposition depths obtained for the validation case.

overtopping at several locations along the channel for the same 25-year maximum mid-future floodevent, as indicated by our simulation results. The channel capacity at all cross sections was also extracted from the DEM following the validation case, where a low daily discharge was used as model input. Satisfactory agreement is obtained between the field-measured channel capacity (green solid line) and the channel capacity obtained from the DEM after the validation test case (blue solid line), with coefficient of correlation (R^2) of 0.635.

The conveyance capacity of the Nakkhu River was also computed from the DEMs at the end of the higher flood scenario simulations. Following the 25-year flood event (solid orange line in Figure 16) the conveyance capacity has significantly reduced from the initial capacity (black solid line), even though the embankments should still be capable of containing the peak flood magnitude of the 25-year flood. However, for the channel geometry extracted from the DEM following the 25-year maximum mid-future flood simulation (solid red line in Figure 16), in-channel deposition has resulted in a further reduction in channel capacity, which is below the 25-year flood discharge at two locations (C7 and C9). The simulated water depths obtained for the 25-year maximum mid-future flood scenario S8 indicate that overtopping and flooding would be likely to occur in the vicinity of these cross-section locations.

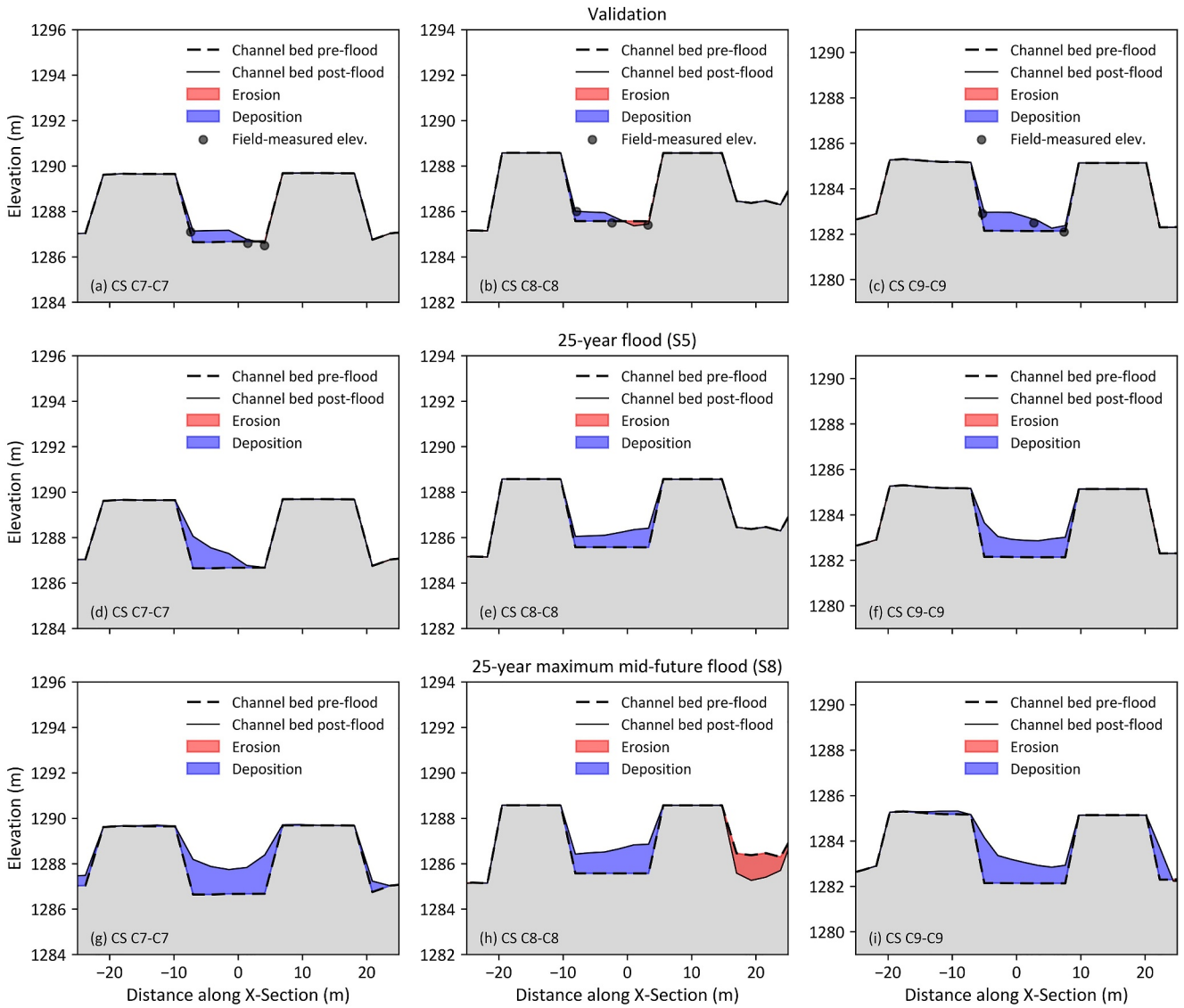

Figure 15. Simulated river cross-section profiles at sections C7 to C9 (middle reach, Figure 2c) for validation case (top row), 25-year (middle row), and 25-year maximum mid-future (bottom row) return period flood events. Black dots represent observed erosion and deposition depths obtained for the validation case.

5. Discussion

5.1. Flood Inundation and Morphology Changes (Erosion/Deposition)

This study examines the complex relationship between river embankments, sediment transport, and flood risk management in the rapidly urbanizing Kathmandu Valley. Embankments effectively reduce flood inundation by 99% for design discharge floods but increase downstream sediment transport by about 32%, altering river morphology. For an extreme 25-year maximum mid-future flood event, the embankments only reduce flooding by 15% while still increasing sediment transport, leading to significant changes in river morphology. River confinement through embankments significantly alters the natural course of a river, leading to a change in its water-sediment characteristics and flow patterns (Cook et al., 2020). Therefore, it is hard to generalize the effectiveness of embankments as a flood control measure, given that their benefits and drawbacks are case-specific.

Inclusion of sediment transport in flood simulation models, particularly when applied to rivers regulated by embankments or flood walls, causes amplification of the consequences of higher return-period flood events. The

10.1029/2024WR037742

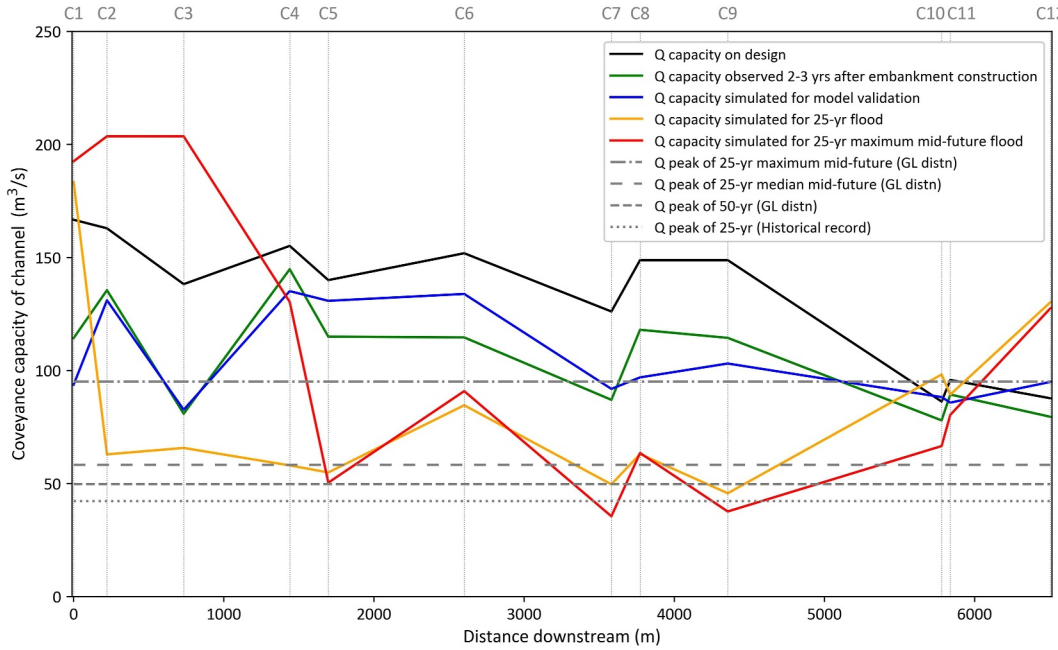

Figure 16. Variation in conveyance capacity along the river channel (at 12 locations, C1–C12) (Figure 2), computed using initial designed channel geometry (black solid line), channel geometry measured 2/3 years after embankment construction (green solid line), simulated conveyance capacity for model validation (blue solid line) and channel capacity after 25-year median (orange solid line) and maximum (red solid line) mid-future floods events. For both cases corresponding to initial and a few years after embankment construction, the computed conveyance capacity is higher than for the 25-year flood event; however, it is not always higher than for the 25-year maximum mid-future flood event. The initially computed conveyance capacity (black solid line) indicates that the river channel can accommodate the 25-year maximum mid-future flood event safely as it propagates downstream up to river cross-section C10 (Figure 2). However, a few years after embankment construction, sediment erosion and deposition processes alter the channel geometry and reduce the channel capacity to pass the same 25-year maximum mid-future flood, with overtopping predicted at many channel sections (green solid line).

change is significant and increases with increasing discharge; for example, flood inundation was five times larger for an extreme flood event (a 25-year maximum mid-future flood) when sediment transport was included in the model (Table 2). In contrast, when the same river was modeled without embankments the impact of including sediment transport decreased as the flood discharge magnitude increased (S. Thapa, Sinclair, Creed, Mudd, et al., 2024). The reason the embanked channel caused increased inundation is the associated reduction in channel conveyance capacity due to sediment aggradation. Other researchers have made similar observations that embanked rivers have a tendency to increase conveyance loss downstream (Ahrendt et al., 2022). In the extreme flood scenario, we attribute the increased morphological change to intense bedload transport. For example, for flood magnitudes up to the 25-year median mid-future event, the percentage of bedload in total sediment transport load is similar to that encountered in previous research (Pratt-Sitaula et al., 2007; Turowski et al., 2010) which found that approximately 35% of the total sediment load in Himalayan rivers, including the Nakkhu River (S. Thapa, Sinclair, Creed, Mudd, et al., 2024), consists of bedload transport. However, in our simulation of a 25-year maximum mid-future flood peak, the proportion changes dramatically, reaching up to 90% bedload contribution to total sediment transport for the embanked river channel (Figures S6 and S7 in Supporting Information S1). Changes in river channel geometry, local slope and the associated increase in velocity are plausible reasons for the increase in bedload transport in the total transported sediment load.

Our results highlight the importance of considering sediment transport in the design of river training structures such as embankments and flood assessments, particularly for the less frequent, higher-intensity flood events. In addition, our research challenges several assumptions of previous research on flood risk, such as assumptions of clear water and channel non-erodibility when implementing two-dimensional (2-D) hydraulic models even for extreme hydrological events (S. Thapa et al., 2020). The present results are in keeping with previous research findings by Guan et al. (2016); S. Thapa, Sinclair, Creed, Mudd, et al. (2024); Nones and Guo (2023), who also highlight the crucial role of sediment in flood dynamics and its importance in flood modeling and flood risk mapping.

Importantly, our results indicate that, following an extreme event, such as the 25-year maximum mid-future flood, the conveyance capacity of the Nakkhu channel could be greatly reduced because of increased in-channel aggradation downstream (Figure 10), to the point that the embankments can no longer contain the design discharge. This finding aligns with conclusions drawn by Slater et al. (2015) who carried out an extensive analysis of 401 rivers across the United States (1950–2013) and showed that geomorphology plays a significant role as a flood hazard driver, and Ahrendt et al. (2022), who demonstrated the significance of variations in channel conveyance in flood hazard dynamics (1930–2020) at 50 river gauges in Western Washington State, USA. These insights emphasize the need to update DEMs regularly after each major flood (which tend to alter the channel geometry), in order to obtain highly accurate flood simulations that account for channel conveyance dynamics within comprehensive flood hazard assessments.

5.2. Risk to Embankment Stability

During our field observations in 2020, 2021, and 2022, we noticed significant under-cutting at multiple locations along the inner wall of the embankments, mostly toward the outer bends of meandering sections, as shown in Figure 8d. During the short time period that has elapsed since these embankments were constructed (2018–2022), no high return-period floods have been observed to date along the Nakkhu River, and the discharge has remained below the design discharge of the embankment. The numerically predicted in-channel erosion was greater than 1 *m* at some outer bends, similar to the field observations. In practice, erosion (Figure 8) poses a serious threat to the stability of an embankment. If unaddressed, erosion could eventually lead to embankment collapse or piping of water under the embankment, posing a threat to the many houses, apartments, and hospital buildings located immediately adjacent to the embankments. This highlights the crucial role of sediment transport in flood dynamics, challenging the assumption that floods below the design discharge of protection structures are negligible (Zischg & Bermúdez, 2020). Upstream surveys revealed instances of seepage and waterlogging (Figure 4b); the waterlogging is higher during the rainy season due to a lack of proper drainage systems, mostly observed in Nepali rivers associated with river embankments Kafle (2021). Bed aggradation is mostly pronounced at channel sections that have smaller slope and larger river meanders; these locations are most prone to overtopping during high magnitude floods, as shown in our simulations (Figure 11). These issues were also reported by the local community during our field campaign. Regular inspections, maintenance, and effective drainage management need to be prioritized after embankments are established. Such measures are critical to mitigate potential risks linked to embankment breaches, overtopping, and/or seepage and to enhance overall flood resilience.

5.3. Implications of Our Research Findings for Future Urban Development

In the current era of rapid urbanization where river channelization, floodplain encroachment, and sediment supply from natural sources and/or human activities are common, our research findings are important in the context of flood management. In Nepal, the conversion of rural administrative units into urban municipalities since 2017 has led to a significant increase in the urban population and accompanied by changes to land-use (Bhattarai et al., 2023; Timsina et al., 2020). In 2019, 16.5 million people, representing 56.5% of Nepal's population, resided in these urban units (Center Bureau of Statistic (CBS), 2021). The corresponding figure was only 22.7% in 2018. The doubling of the urban population from 2018 to 2019 was mainly due to the government's reclassification of rural regions to urban regions. However, these urban regions do not meet internationally accepted norms in terms of requiring basic infrastructure and services, and their development process is not sufficiently flexible to enhance overall quality (Bhattarai et al., 2023; Dixit & Shaw, 2023). Rapid urbanization exerts development pressure on the construction of houses and key infrastructure within floodplains and agricultural areas, leading to more human settlements at increased risk of flooding (Khanal et al., 2019). The development pressure has resulted in widespread implementation of river channelization through embankment-based flood protection schemes in master plans for urban centers to be developed across Nepal. However, such master plans often neglect the impact of riverbed dynamics, posing significant challenges during flood events (Kafle, 2021). Kafle (2021) highlights limitations in designing riverbank protection frameworks in Nepal, particularly in addressing the undercutting of embankments. This demonstrates the necessity of robust river-sensitive urban master plans accounting for riverbed dynamics to ensure comprehensive management of urban rivers (Dixit, 2009; Vaidya & Madan, 2024). The potential impact of increased sediment influx due to sediment mining requires specific attention given that mining has become increasingly commonplace and is sometimes even a prerequisite for embankment

construction. A higher level of sediment influx increases downstream sedimentation and thus promotes overtopping and flood inundation. Our findings provide valuable information for decision-makers in Nepal and elsewhere on the design of flood-protection embankments and the expansion of urban areas on flood plains. Future research should focus on developing holistic approaches that account for the complexities of riverbed dynamics, specially variability in sediment influx, and integrate assessments of future flood risks. Such approaches are crucial in ensuring effective disaster risk management and sustainable urban development in the context of rapid urbanization and its associated challenges.

5.4. Model Uncertainty

A major source of uncertainty in the results from our flood model is associated with the need for multiple parameters, several of which require calibration for each setting. To minimize uncertainty associated with the DEM, we used a recent high-resolution DEM (2 m). To minimize uncertainty introduced by the Manning roughness parameter, we calibrated the model for three constant values of Manning's coefficient that were uniformly distributed over the study reach and used the value which led to suspended sediment concentrations close to field observations.

In future studies, we recommend testing spatially distributed values of the Manning coefficient that better match the local terrain roughness. It would be interesting in a separate study to examine formally uncertainty propagation through the model based on a probability distribution of input Manning coefficient. Although it would be prohibitively expensive in terms of computer resources to undertake this using Monte Carlo simulation, other simpler techniques would be worth considering such as the derived distribution technique following Ang and Tang (1975). A fast approach based on a numerical version of the derived distribution technique is suggested in the papers by Kreitmair et al. (2019); Kreitmair et al. (2020); Sarwar and Borthwick (2023a, 2023b).

A further source of parameter uncertainty arises from the value set for downstream slope, which is required to replicate the backwater effect that occurs at the confluence of the Nakkhu and Bagmati rivers. Although we used field observation data to constrain this parameter, no field data were available for the higher return-period flood events simulated. A flood in the Bagmati river may influence the downstream slope parameter by causing a backwater effect in the Nakkhu river. The value of the downstream slope parameter may therefore need to be adjusted for different magnitude flood events, and should be updated as future observation data become available. Similarly, given the absence of sediment erosion and deposition patterns following extreme events, it is difficult to validate the DEMs of difference for high-magnitude return-period events. As such, the results presented in this study represent possible morphological changes in the embanked Nakkhu River following high flood events. The simulated DEMs of difference do not completely predict the embankment under-cutting values. However, the simulated DEMs of difference can be useful to identify embankment areas susceptible to failure due to undercutting or overtopping exacerbated by riverbed aggradation. The models were run in sediment re-circulation mode because of a lack of information on sediment flux contributed by fine-sediment waste from upstream mining activities and the sediment yield of the upstream catchment at the upper boundary of the study reach. The simulated upstream channel erosion appears slightly higher than expected from field observation for higher return-period flood events. This could be estimated more accurately if upstream sediment influx data were available and used as model input.

6. Conclusions

In Nepal, rapidly increasing urbanization of Kathmandu is leading to floodplain encroachment and increased exposure of communities to flood risk. Climate change, land-use alterations, and alterations to riverbed dynamics caused by sediment transport are amplifying flood risk in urban areas. In response to this growing threat, flood-protection embankments are increasingly being constructed along rivers in developing urban areas in Nepal. This paper has investigated the impact of newly constructed embankments on sediment transport, channel morphology, conveyance capacity, and flood inundation in the Nakkhu River in the Kathmandu basin using a coupled numerical model and a high-resolution DEM. Our analysis of various flood scenarios indicated that Nakkhu River embankments can significantly reduce flood inundation for discharges below the embankment design event compared to the corresponding cases without embankments. It was found that the river embankments could increase downstream sediment transport, altering the river morphology and increasing flood risk during extreme events.

Post-embankment model scenarios with and without sediment transport indicated that alterations in channel geometry due to sedimentation reduced channel capacity and increased downstream flood risk through overtopping, especially where embankments follow sinuous channel patterns. We found that sediment transport does not significantly affect flood inundation (i.e., from 0.0 to 0.3 ha for embanked river channels under flood conditions corresponding to the embankment design discharge; i.e., the 25-year flood event). Sediment transport was found to have a considerable impact on flood inundation, for example, with extent increasing from 5.1 to 24.4 ha for the 25-year maximum mid-future event, which is significantly high for the narrow width channel of 13 m in 6.5 km reach length. The model generated sediment erosion, deposition, and gravel bar formation that were similar to the post-embankment field observations. The predicted sediment erosion along embankments for both high and low return-period flood events raises concern as to the possible undercutting and destabilization of the embankments. Sediment deposition poses a further threat due to reduced conveyance capacity and the potential overtopping of embankments, particularly where backwater effects impact sedimentation.

We recommend integrating sediment transport analysis into the standard design analysis of embankments. It is vital that accurate assessments be made of the impact of embankments on future flood risk affecting new developments on the floodplains. This is particularly important for alluvial rivers carrying high sediment loads. Our findings suggest that embankment construction alone may not always be a sustainable and long-term preventative measure against future floods. Regular inspection and maintenance are necessary to ensure embankment resilience and mitigate risks associated with flood-induced embankment breaches, overtopping, and/or seepage.

Data Availability Statement

The data and software used in this study are openly available, with the following access conditions. Sediment Grain Size Data: collected in the field and available upon Supporting Information S1. The hydro-meteorological data: obtained from the Department of Hydrology and Meteorology (DHM), Nepal, and accessible at the website https://www.dhm.gov.np/hydrology/hms, subject to registration and applicable data fees. The detailed flood return period analysis can be obtained from S. Thapa, Sinclair, Creed, Mudd, et al. (2024); Shrestha et al. (2023), and the same flood magnitude is used for this research. Digital Elevation Models (DEMs): generated from Pleiades data made available by the Committee on Earth Observation Satellites (CNES) within the framework of the Centre National d'Etudes Spatiales (CEOS) Working Group for Disasters. © CNES (2018, 2019, 2020), and Airbus DS, all rights reserved. Commercial use is forbidden. The details of the image IDs used to generate the DEMs are provided in the Supporting Information S1. Landscape Evolution Model (LEM): CAESAR-Lisflood Model (Version 1.9j) used for simulations is available under the GNU General Public License version 3.0 (GPLv3) at the website https://sourceforge.net/projects/caesar-lisflood/files/. River Smoothing Software: conducted using the rgrass7 package in R (version 4.3.1 (2023-06-16 ucrt)), available under the GNU General Public License. The detailed information can be found on the website https://grass.osgeo.org/grass83/manuals/r.carve.html. Figure Generation: created using Matplotlib version 3.5.2 and QGIS Desktop 3.28.1, both under the GNU General Public License (GPL). Simulated Data and Jupyter Notebook Code: the simulated data and Jupyter Notebook code used for generating figures can be accessed at S. Thapa, Sinclair, Creed, Borthwick, et al. (2024).

Acknowledgments
The authors acknowledge the research fund supported by the School of Geosciences, University of Edinburgh, as a part of the UKRI-GCRF funded project Tomorrow's Cities (Grant NE/S009000/1). We thank John Elliott for providing access to the Pleiades data. We thank the Pulchowk Campus, Institute of Engineering (IOE), Nepal, for providing equipment and lab access for analyzing sediment bedload distribution and suspended sediment concentration. Thanks to the Department of Hydrology and Meteorology, Nepal, for providing hydro-meteorological data. The authors are greatly thankful to Simon M. Mudd, Mikael Attal, Bhola N. Ghimire, and Sunil Raut Kshetri for their continuous support, feedback, and encouragement on the research, collecting data, and learning programming languages for data analysis and visualization.

References

Ahrendt, S., Horner-Devine, A. R., Collins, B. D., Morgan, J. A., & Istanbulluoglu, E. (2022). Channel conveyance variability can influence flood risk as much as streamflow variability in western Washington state. *Water Resources Research*, *58*(6), e2021WR031890. https://doi.org/10.1029/2021WR031890

Alfieri, L., Bisselink, B., Dottori, F., Naumann, G., de Roo, A., Salamon, P., et al. (2017). Global projections of river flood risk in a warmer world. *Earth's Future*, *5*(2), 171–182. https://doi.org/10.1002/2016EF000485

Ang, A. H.-S., & Tang, W. H. (1975). *Probability concepts in engineering planning and design, volume i: Basic principles*. John Wiley and Sons, Inc.

Arnell, N. W., & Gosling, S. N. (2016). The impacts of climate change on river flood risk at the global scale. *Climatic Change*, *134*(3), 387–401. https://doi.org/10.1007/s10584-014-1084-5

Aryal, R. K., Lee, B.-K., Karki, R., Gurung, A., Kandasamy, J., Pathak, B. K., et al. (2008). Seasonal pm10 dynamics in Kathmandu valley. *Atmospheric Environment*, *42*(37), 8623–8633. https://doi.org/10.1016/j.atmosenv.2008.08.016

Attal, M., & Lavé, J. (2006). Changes of bedload characteristics along the Marsyandi River (central Nepal): Implications for understanding hillslope sediment supply, sediment load evolution along fluvial networks, and denudation in active orogenic belts. *Special Papers - Geological Society of America*, *398*(09), 143–171. https://doi.org/10.1130/2006.2398(09)

Berz, G. (2000). Flood disasters: Lessons from the past—Worries for the future. *Proceedings of the Institution of Civil Engineers-Water and Maritime Engineering*, *142*(1), 3–8. https://doi.org/10.1680/wame.2000.142.1.3

Bettes, R. (2008). *Sediment transport and alluvial resistance in rivers*. Environment Agency. Retrieved from https://publications.environment-agency.gov.uk/skeleton/publications/ViewPublication.aspx?id=6b5ce931-4211-4143-97ad-a3bd6c70810b

Bhatt, C., Srinivasa Rao, G., Manjushree, P., & Bhanumurthy, V. (2010). Space based disaster management of 2008 Kosi floods, north Bihar, India. *Journal of the Indian Society of Remote Sensing*, *38*(1), 99–108. https://doi.org/10.1007/s12524-010-0015-9

Bhattarai, K., Adhikari, A. P., & Gautam, S. P. (2023). State of urbanization in Nepal: The official definition and reality. *Environmental Challenges*, *13*, 100776. https://doi.org/10.1016/j.envc.2023.100776

Cea, L., & Costabile, P. (2022). Flood risk in urban areas: Modelling, management and adaptation to climate change. A review. *Hydrology*, *9*(3), 50. https://doi.org/10.3390/hydrology9030050

Center Bureau of Statistic (CBS). (2021). *National population and housing Census 2021 report on urban/rural municipality*. National Statistics Office, Government of Nepal. Retrieved from https://censusnepal.cbs.gov.np/results/downloads/urban-rural

Chakraborty, T., Kar, R., Ghosh, P., & Basu, S. (2010). Kosi megafan: Historical records, geomorphology and the recent avulsion of the Kosi River. *Quaternary International*, *227*(2), 143–160. https://doi.org/10.1016/j.quaint.2009.12.002

Chaulagain, D., Rimal, P. R., Ngando, S. N., Nsafon, B. E. K., Suh, D., & Huh, J.-S. (2023). Flood susceptibility mapping of Kathmandu metropolitan city using gis-based multi-criteria decision analysis. *Ecological Indicators*, *154*, 110653. https://doi.org/10.1016/j.ecolind.2023.110653

Cook, K. L., Turowski, J. M., & Hovius, N. (2020). Width control on event-scale deposition and evacuation of sediment in bedrock-confined channels. *Earth Surface Processes and Landforms*, *45*(14), 3702–3713. https://doi.org/10.1002/esp.4993

Coulthard, T. J., Neal, J. C., Bates, P. D., Ramirez, J., de Almeida, G. A., & Hancock, G. R. (2013). Integrating the LISFLOOD-FP 2D hydrodynamic model with the CAESAR model: Implications for modelling landscape evolution. *Earth Surface Processes and Landforms*, *38*(15), 1897–1906. https://doi.org/10.1002/esp.3478

Devkota, L., Crosato, A., & Giri, S. (2012). Effect of the barrage and embankments on flooding and channel avulsion case study Koshi River, Nepal. *Rural Infrastructure*, *3*(3), 124–132.

Dingle, E. H., Creed, M. J., Sinclair, H. D., Gautam, D., Gourmelen, N., Borthwick, A. G. L., & Attal, M. (2020). Dynamic flood topographies in the Terai region of Nepal. *Earth Surface Processes and Landforms*, *45*(13), 3092–3102. https://doi.org/10.1002/esp.4953

Dixit, A. (2009). Kosi embankment breach in Nepal: Need for a paradigm shift in responding to floods. *Economic and Political Weekly*, *44*(6), 70–78. Retrieved from http://www.jstor.org/stable/40278487

Dixit, A., & Shaw, R. (2023). Smart cities in Nepal: The concept, evolution and emerging patterns. *Urban Governance*, *3*(3), 211–218. https://doi.org/10.1016/j.ugj.2023.08.003

Doocy, S., Daniels, A., Murray, S., & Kirsch, T. D. (2013). The human impact of floods: A historical review of events 1980-2009 and systematic literature review. *PLoS Currents*, *5*.

Dottori, F., Szewczyk, W., Ciscar, J.-C., Zhao, F., Alfieri, L., Hirabayashi, Y., et al. (2018). Increased human and economic losses from river flooding with anthropogenic warming. *Nature Climate Change*, *8*(9), 781–786. https://doi.org/10.1038/s41558-018-0257-z

Emerson, D. G., Vecchia, A. V., & Dahl, A. L. (2005). *Evaluation of drainage-area ratio method used to estimate streamflow for the red river of the north basin, North Dakota and Minnesota*. US Department of the Interior, US Geological Survey. https://doi.org/10.3133/sir20055017

Feeney, C. J., Chiverrell, R. C., Smith, H. G., Hooke, J. M., & Cooper, J. R. (2020). Modelling the decadal dynamics of reach-scale river channel evolution and floodplain turnover in CAESAR-Lisflood. *Earth Surface Processes and Landforms*, *45*(5), 1273–1291. https://doi.org/10.1002/esp.4804

Feng, B., Zhang, Y., & Bourke, R. (2021). Urbanization impacts on flood risks based on urban growth data and coupled flood models. *Natural Hazards*, *106*(1), 613–627. https://doi.org/10.1007/s11069-020-04480-0

Fisher, K. (1992). *Morphological effects of river improvement works: Case studies (Tech. Rep.)*. Hydraulics Research Wallingford. Retrieved from http://eprints.hrwallingford.com/id/eprint/326

Gill, P., & Paswan, B. (2018). Sediment and solutions. In *Regional cooperation*. The Third Pole. Retrieved from https://www.thethirdpole.net/en/regional-cooperation/sediment-and-solutions

Graf, E. L., Sinclair, H. D., Attal, M., Gailleton, B., Adhikari, B. R., & Baral, B. R. (2023). Geomorphological and hydrological controls on sediment export in earthquake-affected catchments in the Nepal Himalaya. *EGUsphere*, *2023*, 1–41. https://doi.org/10.5194/egusphere-2022-1347

Guan, M., Carrivick, J. L., Wright, N. G., Sleigh, P. A., & Staines, K. E. (2016). Quantifying the combined effects of multiple extreme floods on river channel geometry and on flood hazards. *Journal of Hydrology*, *538*, 256–268. https://doi.org/10.1016/j.jhydrol.2016.04.004

Hirabayashi, Y., Mahendran, R., Koirala, S., Konoshima, L., Yamazaki, D., Watanabe, S., et al. (2013). Global flood risk under climate change. *Nature Climate Change*, *3*(9), 816–821. https://doi.org/10.1038/nclimate1911

Hudson, P. F., Middelkoop, H., & Stouthamer, E. (2008). Flood management along the Lower Mississippi and Rhine Rivers (The Netherlands) and the continuum of geomorphic adjustment. *Geomorphology*, *101*(1–2), 209–236. https://doi.org/10.1016/j.geomorph.2008.07.001

Institute of Hydrology. (1999). *Flood estimation handbook*.

Ishtiaque, A., Shrestha, M., & Chhetri, N. (2017). Rapid urban growth in the Kathmandu valley, Nepal: Monitoring land use land cover dynamics of a Himalayan city with landsat imageries. *Environments*, *4*(4), 72. https://doi.org/10.3390/environments4040072

Kafle, M. R. (2021). Critical review and improvement of bank protection methods in Nepalese rivers. *Journal of the Institute of Engineering*, *16*(1), 15–25. https://doi.org/10.3126/jie.v16i1.36530

Khanal, N., Uddin, K., Matin, M. A., & Tenneson, K. (2019). Automatic detection of spatiotemporal urban expansion patterns by fusing OSM and landsat data in Kathmandu. *Remote Sensing*, *11*(19), 2296. https://doi.org/10.3390/rs11192296

Kido, R., Inoue, T., Hatono, M., & Yamanoi, K. (2023). Assessing the impact of climate change on sediment discharge using a large ensemble rainfall dataset in Pekerebetsu river basin, Hokkaido. *Progress in Earth and Planetary Science*, *10*(1), 54. https://doi.org/10.1186/s40645-023-00580-0

Kreitmair, M., Adcock, T., Borthwick, A., Draper, S., & Van Den Bremer, T. (2020). The effect of bed roughness uncertainty on tidal stream power estimates for the Pentland Firth. *Royal Society Open Science*, *7*(1), 191127. https://doi.org/10.1098/rsos.191127

Kreitmair, M., Draper, S., Borthwick, A., & Van Den Bremer, T. (2019). The effect of uncertain bottom friction on estimates of tidal current power. *Royal Society Open Science*, *6*(1), 180941. https://doi.org/10.1098/rsos.180941

Kron, W. (2015). Flood disasters–a global perspective. *Water Policy*, *17*(S1), 6–24. https://doi.org/10.2166/wp.2015.001

Lamichhane, S., & Shakya, N. M. (2019). Integrated assessment of climate change and land use change impacts on hydrology in the Kathmandu valley watershed, central Nepal. *Water*, *11*(10), 2059. https://doi.org/10.3390/w11102059

Lane, S. N., Tayefi, V., Reid, S. C., Yu, D., & Hardy, R. J. (2007). Interactions between sediment delivery, channel change, climate change and flood risk in a temperate upland environment. *Earth Surface Processes and Landforms*, *32*(3), 429–446. https://doi.org/10.1002/esp.1404

Leopold, L. B., Wolman, M. G., Miller, J. P., & Wohl, E. E. (2020). *Fluvial processes in geomorphology*. Courier Dover Publications. https://doi.org/10.1016/j.jfranklin.2008.04.005

Li, G. (2003). Ponderation and practice of the yellow river control. *Yellow River Conservancy Press*.

Li, H., Yu, C., Qin, B., Li, Y., Jin, J., Luo, L., et al. (2022). Modeling the effects of climate change and land use/land cover change on sediment yield in a large reservoir basin in the East Asian monsoonal region. *Water*, *14*(15), 2346. https://doi.org/10.3390/w14152346
Li-An, C., Billa, L., & Azari, M. (2018). Anthropocene climate and landscape change that increases flood disasters. *International Journal of Hydrogen Energy*, *2*(4), 487–491. https://doi.org/10.15406/ijh.2018.02.00115
Lihong, W., Shenghui, C., Yuanzheng, L., Hongjie, H., Bikram, M., Vilas, N., et al. (2022). A review of the flood management: From flood control to flood resilience. *Heliyon*, *8*(11), e11763. https://doi.org/10.1016/j.heliyon.2022.e11763
Maharjan, S. B., Steiner, J. F., Shrestha, A. B., Maharjan, A., Nepal, S., Shrestha, M. S., et al. (2021). *The Melamchi flood disaster: Cascading hazard and the need for multihazard risk management*. ICIMOD.
Marahatta, S., Devkota, L., & Aryal, D. (2021). Hydrological modeling: A better alternative to empirical methods for monthly flow estimation in ungauged basins. *Journal of Water Resource and Protection*, *13*(3), 254–270. https://doi.org/10.4236/jwarp.2021.133015
McCann, C. J. (2013). *Urbanization and its effects on channel morphology (Doctoral dissertation, environmental and water resources engineering*. University of Texas at Austin. Retrieved from http://hdl.handle.net/2152/24337
Michaelides, K., & Singer, M. B. (2014). Impact of coarse sediment supply from hillslopes to the channel in runoff-dominated, dryland fluvial systems. *Journal of Geophysical Research: Earth Surface*, *119*(6), 1205–1221. https://doi.org/10.1002/2013JF002959
Montgomery, D. R., & Buffington, J. M. (1997). Channel-reach morphology in mountain drainage basins. *Geological Society of America Bulletin*, *109*(5), 596–611. https://doi.org/10.1130/0016-7606(1997)109%3C0596:CRMIMD%3E2.3.CO;2
Morris, M., Hanson, G., & Hassan, M. (2008a). Improving the accuracy of breach modelling: Why are we not progressing faster? *Journal of Flood Risk Management*, *1*(3), 150–161. https://doi.org/10.1111/j.1753-318X.2008.00017.x
Morris, M., Hassan, M., Kortenhaus, A., Geisenhainer, G., Visser, P., & Zhu, Y. (2008b). Modelling breach initiation and growth. In *Flood Risk Management - Research and Practice Proceedings of Floodrisk Conference 2008*. Retrieved from http://eprints.hrwallingford.com/id/eprint/700
Muzzini, E., & Aparicio, G. (2013). *Urban growth and spatial transition in Nepal: An initial assessment*. World Bank Publications. https://doi.org/10.1596/978-0-8213-9659-9
Nones, M., & Guo, Y. (2023). Can sediments play a role in river flood risk mapping? Learning from selected European examples. *Geo-environmental Disasters*, *10*(1), 20. https://doi.org/10.1186/s40677-023-00250-9
Oberhagemann, K., Haque, A. M. A., & Thompson, A. (2020). A century of riverbank protection and river training in Bangladesh. *Water*, *12*(11), 3018. https://doi.org/10.3390/w12113018
Ouellet, C., Saint-Laurent, D., & Normand, F. (2012). Flood events and flood risk assessment in relation to climate and land-use changes: Saint-François River, Southern Québec, Canada. *Hydrological Sciences Journal*, *57*(2), 313–325. https://doi.org/10.1080/02626667.2011.645475
Pekel, J. F., Cottam, A., Gorelick, N., & Belward, A. S. (2016). High-resolution mapping of global surface water and its long-term changes. *Nature*, *540*(7633), 418–422. https://doi.org/10.1038/nature20584
Pfeiffer, A. M., Collins, B. D., Anderson, S. W., Montgomery, D. R., & Istanbulluoglu, E. (2019). River bed elevation variability reflects sediment supply, rather than peak flows, in the uplands of Washington state. *Water Resources Research*, *55*(8), 6795–6810. https://doi.org/10.1029/2019WR025394
Pokhrel, B. K. (2018). Impact of land use change on flow and sediment yields in the Khokana outlet of the Bagmati River, Kathmandu, Nepal. *Hydrology*, *5*(2), 22. https://doi.org/10.3390/hydrology5020022
Pratt-Sitaula, B., Garde, M., Burbank, D. W., Oskin, M., Heimsath, A., & Gabet, E. (2007). Bedload-to-suspended load ratio and rapid bedrock incision from Himalayan landslide-dam lake record. *Quaternary Research*, *68*(1), 111–120. https://doi.org/10.1016/j.yqres.2007.03.005
Ramirez, J. A., Zischg, A. P., Schürmann, S., Zimmermann, M., Weingartner, R., Coulthard, T., & Keiler, M. (2020). Modeling the geomorphic response to early river engineering works using CAESAR-Lisflood. *Anthropocene*, *32*, 100266. https://doi.org/10.1016/j.ancene.2020.100266
Raven, E. K., Lane, S. N., & Bracken, L. J. (2010). Understanding sediment transfer and morphological change for managing upland gravel-bed rivers. *Progress in Physical Geography: Earth and Environment*, *34*(1), 23–45. https://doi.org/10.1177/0309133309355631
Rentschler, J., Salhab, M., & Jafino, B. A. (2022). Flood exposure and poverty in 188 countries. *Nature Communications*, *13*(1), 3527. https://doi.org/10.1038/s41467-022-30727-4
Sampson, C. C., Smith, A. M., Bates, P. D., Neal, J. C., Alfieri, L., & Freer, J. E. (2015). A high-resolution global flood hazard model. *Water Resources Research*, *51*(9), 7358–7381. https://doi.org/10.1002/2015WR016954
Sarwar, S., & Borthwick, A. G. (2023a). Characterization of uncertainty in maximum tidal elevation near Bangladesh coastline due to uncertain sea level rise. *Journal of Flood Risk Management*, *16*(4), e12935. https://doi.org/10.1111/jfr3.12935
Sarwar, S., & Borthwick, A. G. (2023b). Estimate of uncertain cohesive suspended sediment deposition rate from uncertain floc size in Meghna Estuary, Bangladesh. *Estuarine, Coastal and Shelf Science*, *281*, 108183. https://doi.org/10.1016/j.ecss.2022.108183
Sharma, T. P. P., Zhang, J., Koju, U. A., Zhang, S., Bai, Y., & Suwal, M. K. (2019). Review of flood disaster studies in Nepal: A remote sensing perspective. *International Journal of Disaster Risk Reduction*, *34*, 18–27. https://doi.org/10.1016/j.ijdrr.2018.11.022
Shiono, K., Chan, T. L., Spooner, J., Rameshwaran, P., & Chandler, J. H. (2009). The effect of floodplain roughness on flow structures, bedforms and sediment transport rates in meandering channels with overbank flows: Part i. *Journal of Hydraulic Research*, *47*(1), 5–19. https://doi.org/10.3826/jhr.2009.2944-I
Shrestha, D., Basnyat, D. B., Gyawali, J., Creed, M. J., Sinclair, H. D., Golding, B., et al. (2023). Rainfall extremes under future climate change with implications for urban flood risk in Kathmandu, Nepal. *International Journal of Disaster Risk Reduction*, *97*, 103997. https://doi.org/10.1016/j.ijdrr.2023.103997
Sinha, R. (2008). Kosi: Rising waters, dynamic channels and human disasters. *Economic and Political Weekly*, *43*, 42–46. Retrieved from https://www.jstor.org/stable/40278180
Sinha, R., Gupta, A., Mishra, K., Tripathi, S., Nepal, S., Wahid, S., & Swarnkar, S. (2019). Basin-scale hydrology and sediment dynamics of the Kosi River in the Himalayan foreland. *Journal of Hydrology*, *570*, 156–166. https://doi.org/10.1016/j.jhydrol.2018.12.051
Slater, L. J., Singer, M. B., & Kirchner, J. W. (2015). Hydrologic versus geomorphic drivers of trends in flood hazard. *Geophysical Research Letters*, *42*(2), 370–376. https://doi.org/10.1002/2014GL062482
Smith, A., Sampson, C., & Bates, P. (2015). Regional flood frequency analysis at the global scale. *Water Resources Research*, *51*(1), 539–553. https://doi.org/10.1002/2014WR015814
Stover, S., & Montgomery, D. (2001). Channel change and flooding, Skokomish River, Washington. *Journal of Hydrology*, *243*(3–4), 272–286. https://doi.org/10.1016/S0022-1694(00)00421-2
Thapa, R. B., & Murayama, Y. (2012). Scenario based urban growth allocation in Kathmandu valley, Nepal. *Landscape and Urban Planning*, *105*(1–2), 140–148. https://doi.org/10.1016/j.landurbplan.2011.12.007

Thapa, S., Creed, M., Sinclair, H., Mudd, S., Attal, M., Muthusamy, M., & Ghimire, B. N. (2022). Modelling the impact of sediment grain size on flooding in the Kathmandu basin, Nepal. In *39th IAHR World Congress: From Snow to Sea* (pp. 784–794). https://doi.org/10.3850/IAHR-39WC2521711920221802

Thapa, S., Shrestha, A., Lamichhane, S., Adhikari, R., & Gautam, D. (2020). Catchment-scale flood hazard mapping and flood vulnerability analysis of residential buildings: The case of Khando River in Eastern Nepal. *Journal of Hydrology: Regional Studies*, *30*, 100704. https://doi.org/10.1016/j.ejrh.2020.100704

Thapa, S., Sinclair, H. D., Creed, M. J., Borthwick, A. G. L., Watson, C. S., & Muthusamy, M. (2024). Sediment transport and flood risk: Impact of newly constructed embankments on river dynamics and flooding in Kathmandu, Nepal, [Dataset]. School of GeoSciences, University of Edinburgh. https://doi.org/10.7488/ds/7806

Thapa, S., Sinclair, H. D., Creed, M. J., Mudd, S. M., Attal, M., Borthwick, A. G. L., et al. (2024). The impact of sediment flux and Calibre on flood risk in the Kathmandu valley, Nepal. *Earth Surface Processes and Landforms*, *49*(2), 706–727. https://doi.org/10.1002/esp.5731

Timsina, N. P., Shrestha, A., Poudel, D. P., & Upadhyaya, R. (2020). Trend of urban growth in Nepal with a focus in Kathmandu valley: A review of processes and drivers of change UKRI GCRF urban disaster risk Hub. https://doi.org/10.7488/era/722

Turowski, J. M., Rickenmann, D., & Dadson, S. J. (2010). The partitioning of the total sediment load of a river into suspended load and bedload: A review of empirical data. *Sedimentology*, *57*(4), 1126–1146. https://doi.org/10.1111/j.1365-3091.2009.01140.x

United Nations. (2019). *World urbanization prospects: The 2018 revision*. United Nations. Retrieved from https://population.un.org/wup/Publications/Files/WUP2018-Report.pdf(ST/ESA/SER.A/420)

Vaidya, H., & Madan, N. (2024). Chapter 4 - Mainstreaming River thinking into urban planning. In V. R. Shinde, R. R. Mishra, U. Bhonde, & H. Vaidya (Eds.), *Managing Urban Rivers* (pp. 57–71). Elsevier. https://doi.org/10.1016/B978-0-323-85703-1.00011-0

Vázquez-Tarrío, D., Ruiz-Villanueva, V., Garrote, J., Benito, G., Calle, M., Lucía, A., & Díez-Herrero, A. (2023). Effects of sediment transport on flood hazards: Lessons learned and remaining challenges. *Geomorphology*, *446*, 108976. https://doi.org/10.1016/j.geomorph.2023.108976

Wang, S. W., Gebru, B. M., Lamchin, M., Kayastha, R. B., & Lee, W.-K. (2020). Land use and land cover change detection and prediction in the Kathmandu district of Nepal using remote sensing and gis. *Sustainability*, *12*(9), 3925. https://doi.org/10.3390/su12093925

Ward, P. J., Jongman, B., Weiland, F. S., Bouwman, A., van Beek, R., Bierkens, M. F. P., et al. (2013). Assessing flood risk at the global scale: Model setup, results, and sensitivity. *Environmental Research Letters*, *8*(4), 044019. https://doi.org/10.1088/1748-9326/8/4/044019

Wilcock, P. R., & Crowe, J. C. (2003). Surface-based transport model for mixed-size sediment. *Journal of Hydraulic Engineering*, *129*(2), 120–128. https://doi.org/10.1061/(ASCE)0733-9429(2003)129:2(120)

World Bank. (2014). *The Ganges strategic basin assessment: A discussion of regional opportunities and risks - World Bank South Asia regional report: Main report*. World Bank Group. Retrieved from http://documents.worldbank.org/curated/en/955751468000263739/Main-report

Yang, Q., Zheng, X., Jin, L., Lei, X., Shao, B., & Chen, Y. (2021). Research progress of urban floods under climate change and urbanization: A scientometrics analysis. *Buildings*, *11*(12), 628. https://doi.org/10.3390/buildings11120628

Yilmaz, M. U., & Onoz, B. (2020). A comparative study of statistical methods for daily streamflow estimation at ungauged basins in Turkey. *Water*, *12*(2), 459. https://doi.org/10.3390/w12020459

Zischg, A. P., & Bermúdez, M. (2020). Mapping the sensitivity of population exposure to changes in flood magnitude: Prospective application from local to global scale. *Frontiers in Earth Science*, *8*, 390. https://doi.org/10.3389/feart.2020.534735